# 5

# Emission fields and antenna systems

The purpose of this chapter is to consider the basic characteristics of the emission field of natural objects and the physical features of receiving the emission by microwave antenna complexes. Using the method of equivalent circuits, the basic notions of brightness and antenna temperatures are introduced, which have been widely used in the theory and practice of passive microwave remote sensing and in radio-astronomy. The basic data on radio-astronomical instruments and antenna complexes are presented. On the basis of spatial-spectral notions, the antenna smoothing equation is introduced and the procedures of restoring radiothermal images are analysed. On the basis of passive microwave remote sensing experience, the basic methods of measuring the parameters and calibrations of onboard antenna systems are introduced and analysed.

## 5.1 BASIC CHARACTERISTICS OF THE EMISSION FIELD

The analysis of radiative transfer in natural media essentially differs from the standard formulation of the problem of propagation of waves in electromagnetism as planar waves (see section 1.6). This is, first of all, due to the fact, that at each point of the medium (or of the medium's surface) the propagation of emission cannot be represented by a single vector. In order to characterize the emission falling on a given point, it is necessary to know the emission from all directions and, in addition, it is important to take into account the solid angles from which the external radiation falls on an elementary volume, and the solid angle from which the observation and recording of emission will be carried out. For this reason, to describe the amount of radiation energy transferred in the given direction per unit time and inside an infinitesimal solid angle, in remote sensing, astrophysics and heat exchange problems a fundamental physical quantity is introduced, which is called the spectral (monochromatic) radiation intensity. This quantity is introduced in a

strictly differential form, and then, on its basis, a spectrum of integral quantities is introduced which are widely used in the theory and practice of remote sensing, in astrophysics and radio-astronomy, as well as in heat exchange problems (Troitskii, 1954; Chandrasekhar, 1960; Sobolev, 1963; Siegel and Howell, 1972; Ozisik, 1973; Marchuk, 1976; Ulaby *et al.*, 1981, 1982, 1986; Kondratyev *et al.*, 1995; Apresyan and Kravtsov, 1996; Thomas and Stamnes, 1999).

### 5.1.1 Spectral intensity

For the determination of spectral intensity we shall consider the elementary area $dA$ around the point of space with coordinate $\mathbf{r}$, which is characterized by unit vector $\mathbf{n}$ in the direction to a normal (Figure 5.1). Let $dE_\nu$ be the quantity of the energy of radiation in the frequency band between $\nu$ and $\nu + d\nu$, which propagates inside an infinitesimal solid angle $d\Omega$ in the direction of vector $\mathbf{\Omega}$ and passes through the elementary area $dA$ (here we have in mind the total radiation, i.e. the external radiation passing through the area and the thermal radiation of the object, as well as the radiation reflected by the area) for the time interval from $t$ to $t + dt$. Designate by $\theta$ the polar angle between the unit vector $\mathbf{n}$ and the radiation propagation direction $\mathbf{\Omega}$. The spectral radiation intensity $I_\nu(\mathbf{r}, \Omega, t)$ is defined as the following limit:

$$I_\nu(\mathbf{r}, \mathbf{\Omega}, t) = \lim_{dA, d\Omega, d\nu, dt \to 0} \left[ \frac{dE_\nu}{dA \cos\theta \, d\Omega \, d\nu \, dt} \right]. \tag{5.1}$$

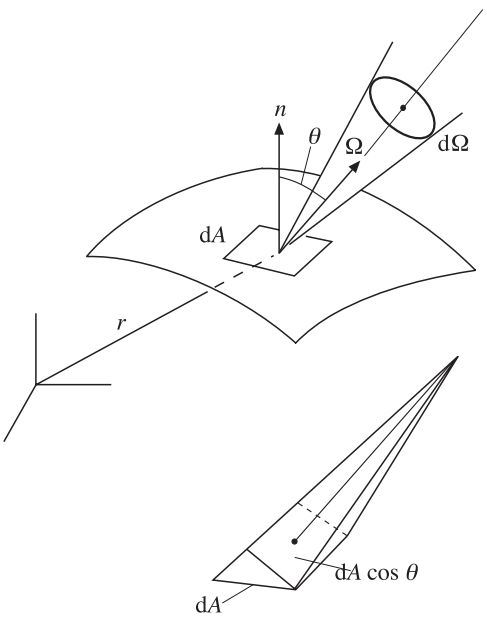


**Figure 5.1.** System of axes for the determination of spectral intensity. See explanations of designations in the text.

In this expression $dA\cos\theta$ is the projection of surface $dA$ on the plane perpendicular to direction $\mathbf{\Omega}$. Note that in this definition the intensity is determined in terms of a surface projection on the observation direction $\mathbf{\Omega}$. The determination of radiation intensity with respect to the surface element area (as was done here) has an important physical advantage, namely, the equal intensity of emission of an ideal black body in all directions (see, for example, Siegel and Howell, 1972). Of course, the intensity of natural objects depends on the radiation propagation direction, and for this reason the functional dependence on the observation direction $\mathbf{\Omega}$ is introduced into definition (5.1). Generally speaking, the angular dependencies of radiation intensity are, as we shall see soon, a very important information parameter for determining the physical properties of objects from remote measurement data.

According to expression (5.1), the spectral intensity is equal to the amount of radiation energy (in appropriate units, see Appendix A) passing through a unit area perpendicular to the propagation direction $\mathbf{\Omega}$, inside a unit solid angle whose axis coincides with direction $\mathbf{\Omega}$, in a unit frequency band which includes the working frequency $\nu$, and per the unit of time.

The dimension of the quantity considered in the SI system is $\mathrm{W\,m^{-2}\,Hz^{-1}\,sr}$.

If the radiation intensity emitted by the surface element or falling on it, is considered within the finite frequency band, lying between $\nu_1$ and $\nu_2$ and inside the solid angle concluded between $\Omega_1(\theta_1, \varphi_1)$ and $\Omega_2(\theta_2, \varphi_2)$, then the quantity

$$\int_{\nu_1}^{\nu_2}\int_{\varphi_1}^{\varphi_2}\int_{\theta_1}^{\theta_2} I_\nu(\mathbf{r}, \theta, \varphi, t)\cos\theta\sin\theta\,d\theta\,d\varphi\,d\nu \tag{5.2}$$

represents the amount of radiation energy, falling on a unit surface area or emitted by it per unit time, within the frequency band from $\nu_1$ to $\nu_2$ inside the solid angle from $\Omega_1$ to $\Omega_2$. The elementary solid angle $d\Omega$ in polar coordinates equals

$$d\Omega = \sin\theta\,d\theta\,d\varphi, \tag{5.3}$$

where $\theta$ is the polar angle between the emission direction and the normal to the surface, and $\varphi$ is the azimuthal angle around the normal. Then expression (5.2) can be presented in the following standard form:

$$\int_{\nu_1}^{\nu_2}\int_{\varphi_1}^{\varphi_2}\int_{\mu_1}^{\mu_2} I_\nu(r, \mu, \varphi, t)\mu\,d\mu\,d\varphi\,d\nu, \tag{5.4}$$

where $\mu = \cos\theta$.

In optics, astronomy and radio-astronomy the considered characteristic is called the brightness of a physical object (Prochorov, 1984).

If this characteristic is considered throughout the range of positive frequencies, then it is called the total radiation intensity.

### 5.1.2 Spectral radiation flux

In determining this quantity, of importance is the radiation flux vector (or power flux vector) $\mathbf{q}_\nu(\mathbf{r})$, which is obtained by integrating the quantity $\mathbf{\Omega} I_\nu(\mathbf{r}, \mathbf{\Omega})$ over the

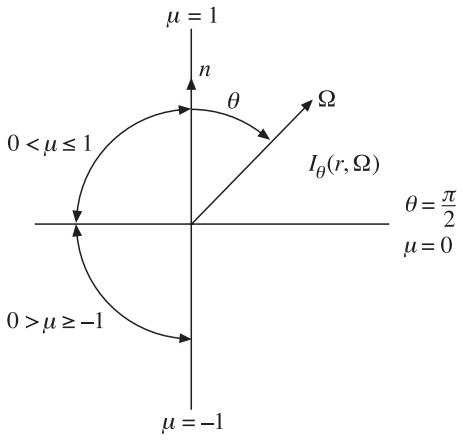


**Figure 5.2.** System of axes for resulting emission flow. See text for explanations of the designations.

spherical solid angle

$$\mathbf{q}_\nu(\mathbf{r}) = \int_{\Omega=4\pi} I_\nu(\mathbf{r}, \mathbf{\Omega})\mathbf{\Omega}\, d\Omega. \tag{5.5}$$

In studying natural surfaces and making various types of antenna measurements, of importance is the knowledge of a component of this vector in the given particular direction **n**. This quantity is called the net radiation flux in the given direction **n** and is determined as a scalar product of vectors $\mathbf{q}_\nu(\mathbf{r})$ and **n**:

$$q_{\nu n}(\mathbf{r}) = \mathbf{n} \cdot \mathbf{q}_\nu(\mathbf{r}) = \int_{\Omega=4\pi} I_\nu(\mathbf{r}, \mathbf{\Omega})(\mathbf{\Omega} \cdot \mathbf{n})\, d\Omega \tag{5.6}$$

Let $\theta$ be the polar angle between directions $\mathbf{\Omega}$ and **n** (Figure 5.2). Then the scalar product of vectors is equal to the cosine of polar angle, and expression (5.6) will take the form:

$$q_{\nu n}(r) = \int_{\varphi=0}^{2\pi} \int_{\mu=-1}^{+1} I_\nu(\mathbf{r}, \mu, \varphi)\mu\, d\mu\, d\varphi. \tag{5.7}$$

Here $q_{\nu n}(\mathbf{r})$ is the density of the net radiation flux through the unit of area perpendicular to direction **n**, per time unit, in a unit frequency band, formed by radiation falling from all directions within the limits of a spherical solid angle. Recalling the physical interpretation of Poynting's vector (Stratton, 1941; and see also section 1.6) as the density of the energy flux at any point of the field intersecting a unit area, whose normal is oriented in the direction of vector $[\mathbf{E}\,\mathbf{H}]$, the quantity $q_{\nu n}(\mathbf{r})$ can be interpreted as the magnitude of Poynting's vector of resulting radiation intersecting a unit area with the normal **n**.

In studying the radiation of natural surfaces and various types of radio sources, the 'radiation flux' term is often used to characterize a unidirectional flux of electromagnetic energy. It corresponds to expression (5.7), in which the integral is taken

over the directions lying on the same side of an area (one-sided ozone-directional flux). In astronomy such a quantity is called the brightness in a unit frequency band, and the net flux through an area equals the difference of one-sided fluxes on both sides of an area.

The dimension of the considered quantity is $\mathrm{Wm^{-2}\,Hz^{-1}}$. In radio-astronomy the quantity equal to $10^{-26}\,\mathrm{Wm^{-2}\,Hz^{-1}}$ is called the flux unit, or jansky = Jy (see Appendix A).

In the equilibrium radiation field (for example, inside the thermostat) the net radiation flux through any surface area is zero. This result can easily be obtained from expression (5.7), if we substitute there the value of intensity which does not depend on the direction.

If the question is of the one-directional flux of the black-body radiation into free space from a unit surface, then in this case the expression for a flux will be written as

$$q_{\nu n}(\mathbf{r}) = \int_{\varphi=0}^{2\pi} \int_{\mu=0}^{+1} I_\nu(\mathbf{r}, \mu, \varphi)\mu \, \mathrm{d}\mu \, \mathrm{d}\varphi, \tag{5.8}$$

and in the case where the radiation does not depend on direction, i.e. $I_\nu(\mathbf{r}, \mathbf{\Omega}, t) = I_{\nu 0}$, the expression for one-directional flux will be equal to

$$q_{\nu n}(\mathbf{r}) = \pi I_{\nu 0}(\mathbf{r}). \tag{5.9}$$

The relation obtained is called Lambert's cosine law. It has been widely applied both in theoretical works (the ideal light-scattering scheme and the ideal black-body radiation scheme), and in microwave remote sensing practice as the characteristic of an ideal black-body emitter in calibration operations.

We pay attention to one more important circumstance. On the basis of a reciprocity theorem, proved in Maxwellian electromagnetism (Stratton, 1941; Slater, 1942; Alpert *et al.*, 1953), it can be shown that the electromagnetic characteristics of emitting objects have the same form and quantitative values as if the same objects were to absorb the electromagnetic energy. Thus, the characteristics considered above can equally be related both to emitting objects (the terrestrial surfaces and radio sources) and to the objects absorbing the external electromagnetic energy (antenna systems, for instance).

If this characteristic is considered throughout the range of positive frequencies, then it is called the total intensity flux.

### 5.1.3 Spectral radiant energy density

The element of the medium's volume, in which the complicated radiation processes take place, contains at each time instant some particular amount of radiation energy, which falls on it from all directions within the limits of a spherical solid angle. The amount of electromagnetic radiation energy contained in a unit volume, in a unit frequency band, is called the spectral radiant energy density and is designated by symbol $u_\nu(\mathbf{r})$.

The relationship between the spectral radiant energy density of the electromagnetic field and Poynting's vector has already been established by ourselves for the

mode of planar waves in the form of (1.19). Using this relationship and taking into account the circumstance that the radiation of intensity $I(\mathbf{r}, \mathbf{\Omega})$ falls on the volume's element from all directions, the spectral radiant energy density is determined by the following expression:

$$u_\nu(\mathbf{r}) = \frac{1}{c} \int_{\varphi'=0}^{2\pi} \int_{\mu'=-1}^{+1} I_\nu(\mathbf{r}, \mu', \varphi') \, \mathrm{d}\mu' \, \mathrm{d}\varphi', \tag{5.10}$$

where $c$ is the radiation propagation velocity in a medium. For dielectric transparent media with the index of refraction $n$ the expression (5.10) takes the form:

$$u_\nu(\mathbf{r}) = \frac{n}{c_0} \int_{\varphi'=0}^{2\pi} \int_{\mu'=-1}^{+1} I_\nu(\mathbf{r}, \mu', \varphi') \, \mathrm{d}\mu' \, \mathrm{d}\varphi'. \tag{5.11}$$

In an equilibrium radiation field (for example, the radiation inside the thermostat) expression (5.11) is reduced to the well-known form:

$$u_\nu(\mathbf{r}) = \frac{4\pi n}{c_0} I_\nu(\mathbf{r}). \tag{5.12}$$

We shall repeatedly use this expression hereafter in considering the thermal radiation laws (Planck's formula and Kirchhoff's law) (Chapter 6).

The integral spectral radiant energy density $u(\mathbf{r})$ is obtained by integration of $u_\nu(\mathbf{r})$ over positive frequencies:

$$u(\mathbf{r}) = \int_0^\infty u_\nu(\mathbf{r}) \, \mathrm{d}\nu. \tag{5.13}$$

In general, we note, that the processes of scattering, absorption and emission by the element of volume and by the element of surface of natural media are very complicated. Therefore, in the scientifice and technical literature different approaches and definitions are used for describing the processes of the interaction of electromagnetic waves with volume and surface elements of the medium under study. The discussion of these concepts is beyond the framework of this book. We shall introduce and consider some additional definitions as they are required. An in-depth analysis of basic concepts can be found in a series of fundamental works (Chandrasekhar, 1960; Sobolev, 1963; Siegel and Howell, 1972; Ozisik, 1973).

## 5.2 MICROWAVE ANTENNAS AND THEIR CHARACTERISTICS

As we have noted, the most important function of the antenna system consists in forming the radiation with strictly defined and prespecified characteristics. According to the reciprocity theorem, in electrodynamics any antenna system can be used both for receiving the electromagnetic signal, and for emitting it with the same spatial-angular characteristics. We shall utilize this circumstance quite often hereafter, without additional explanation.

### 5.2.1 Emission of radiowaves

The emission of electromagnetic waves is associated with the process of emission by oscillating electrical charges, the simplest emitter being the electrical (or magnetic) dipole of length $l \ll \lambda$ and oscillation frequency $\omega$.

At distances $r < \lambda$ the field can be considered to be quasi-static and rapidly decreasing with distance as $r^{-2}$ and $r^{-3}$ (the induction fields). The emission of energy cannot be associated with such fields. The energy flux, flowing through the unit area per unit time, is expressed by Poynting's vector component perpendicular to this area. In quasi-static fields **E** and **H** are shifted in phase by $\pi/2$, as it takes place in standing waves. As a result, Poynting's vector, while oscillating with a double frequency, time-averaged in the period is exactly equal to zero. As we have noted above (section 1.6), the distinction of Poynting's vector from zero can be caused only by fields **E** and **H**, which oscillate with equal phase (as in running waves) and decrease in proportion to $1/r$ (and, accordingly, the Poynting's vector magnitude decreases as $1/r^2$). It is interesting to note that the latter conclusion follows directly from the energy conservation law, since in the absence of losses in a medium the total energy flux in space (the source power) should not change with the distance. And since the area of closed surfaces, enveloping the source of electromagnetic radiation, grows as $r^2$, it is necessary, that the magnitude of Poynting's vector be proportional to $r^{-2}$. Thus, the field of a source in the near zone is some kind of a preliminary phase under generation of running fields responsible for radiation and carrying remote information about a physical object.

One more important point is associated with the representation of the total power which is absorbed by the antenna element from incident radiation. Using the impedance method (section 1.6), the total power received by an antenna element can be presented as the power absorbed in some active resistance, which is called the radiation resistance. As we have already noted, the increase of antenna operation efficiency, and, accordingly, the maximum power received from ambient space, can be assured under the regime of 'match' between the wave resistance of space and the input resistance of a measuring device. It is just this procedure which is performed by the antenna system.

### 5.2.2 Antenna directional pattern (ADP)

The important function of the antenna system consists in forming the radiation with particular and prespecified characteristics and, first of all, with the specified directional pattern, i.e. with the angular distribution (in three-dimensional space) of the radiation field amplitude. Along with the amplitude pattern, the power gain pattern is often used. This is the angular distribution of the radiation energy flux density (the Poynting's vector magnitude or the intensity of emission in the given direction) of the antenna in the far zone (the emission zone). For antennas of complicated configuration both these directional patterns have a multi-lobed structure, which is caused by the interference of waves emitted and scattered by various antenna elements. If the fields of all elements are added in synchronous

phase, then the corresponding maximum is called the main lobe. The directional pattern is depicted in various forms – as a three-dimensional, relief picture; as a planimetric map with the lines of equal levels, or by means of separate planar cross-sections, or more often by two orthogonal cross-sections passing through the direction of a major maximum and **E** and **H** vectors. Since the main part of the power emitted or received by an antenna is localized within the main lobe, the antenna emission directivity is characterized by the antenna beamwidth at half-maximum points (the 3 dB width) at the half power level $\theta_{0.5}$ (or $\theta_{3\text{dB}}$) or at zero level $\theta_0$ (at zero points). The majority of beam antennas are shown to satisfy the $\theta_0 \cong 2.5\,\theta_{0.5}$ relation, which is widely used in observational practice. The $\theta_{0.5}$ quantity determines the linear angular resolution of an antenna and can be approximately estimated by the following formula (in radians):

$$\theta_{3\text{dB}} \approx 1.22\frac{\lambda}{D}, \tag{5.14}$$

where $D$ is the geometric size (the aperture) of the antenna at the given cross-section of the directional pattern. This relation coincides with Rayleigh's criterion, which is used in optics for evaluating the resolution capability of optical systems (Born and Wolf, 1999; Mandel and Wolf, 1995). This criterion makes it possible to determine numerically the resolution capability of an instrument by using a sample double source: at the angular distance between components, lower than $\theta_{0.5}$, the diffraction images of components merge into a single maximum. The quantitative characteristic considered is purely geometrical and only testifies to the possibility of obtaining the appropriate detailed structure of an image. However, the possibility of restoring the true brightness distribution over a studied object from the smoothed images obtained by an antenna represents a separate specific problem, which is stipulated, first of all, by the relation between the useful signal and noise components. In the so-called super-beam antennas this limitation is overcome either by producing some specific, sharply oscillating background distribution in the aperture (unstable to the lowest fluctuations), or by introducing some additional model presentations of a studied object into the restoration procedure. As the $D/\lambda$ ratio decreases, the antenna directional pattern broadens. However, even for an extremely small antenna (the elementary emitter) the directional pattern is not fully isotropic (unlike the elementary acoustic emitters). For example, the directional pattern of electrical and magnetic dipoles has the form of a toroid whose axis coincides with the dipole axis (Born and Wolf, 1999).

In order to quantitatively understand the situation with the angular resolution in a microwave band, we shall estimate the diameter of an antenna aperture (at the working wavelength of 1 cm) required for obtaining, with its help, a resolution capability equal to the resolution of the human eye (1 minute of arc). Substituting these values into formula (5.14), we obtain that the aperture diameter must be very great, namely, 42 m. The design and manufacture of antennas of such a size is a very complicated and costly procedure.

When it is necessary to obtain higher resolutions (than those determined by Rayleigh's criterion), investigators resort to a method which differs from the

mechanical increase of the aperture size. This method consists in producing a set of sparse-aperture antennas with a specialized system of processing. Such systems are called radio interferometers; they can be manufactured both in ground-based, and in onboard versions (Esepkina *et al.*, 1973; Matveenko *et al.*, 1983; Ruf, 1999; Kardashiov, 2000; Rosolen *et al.*, 1999). Under ground conditions another approach is also applied, namely, the arranging of a set of a great number of closely placed small antennas with a complex (and rigid) system of electrical linkage between them. Such systems are called cophased beam arrays, and they are, apparently, a major modern development in ground-based radio-astronomy (Feder, 2000; Parfitt *et al.*, 2000). There have also been some attempts at producing very large (up to 500 metres in diameter) mechanical mirrors situated in geological folds of the Earth's surface (the so-called Arecibo-style dish) (Peng and Nan, 2002). As far as onboard systems are concerned, then, taking into account the flying vehicle's motion over the surface being investigated, it is also possible to sharply increase the resolution capability by accumulating the thermal signal received; i.e. some kind of a synthetic aperture microwave radiometry is formed in this case (Milman, 1988; Ruf *et al.*, 1988; Camps *et al.*, 1998; Goutoule and de Boer, 2000; Dong *et al.*, 2000; Wu *et al.*, 2000).

The structure of the field of systems of emitters depends on their mutual position, on the general configuration of a system, on phase and amplitude relations between the currents in elementary emitters, on the availability and arrangement of non-emitting (passive, structural) components, etc. However, a common factor is the circumstance that, at a distance from the aperture plane equal to several wavelengths (in the wave zone), the rapidly decreasing fields of induction become insignificant, and the radiation field is determined by a superposition of fields excited by emitters. It is important to note that the presence of structural components in the radiation field of antenna systems greatly influences the side-lobe area, whereas the shape of a main lobe is not sensitive to the form of the basic aperture or to the presence of various structural components. Physically, this is associated with the fact that the formation of side lobes is the result of the interference of edge waves (in accordance with the Huygens–Fresnel principle) over the directions which represent the lines of constant value of the phase difference of edge waves (a hyperbola). It is important to note also that the formation of side lobes already takes place in the near field of antenna emission (the Fresnel zone), whereas the main lobe is formed in the far zone (the Fraunhofer zone) only. This pattern is demonstrated qualitatively in Figure 5.3.

The spatial evolution of the antenna emission field, generated by the broad synphase aperture, is shown conventionally in Figure 5.3 under an assumption of sufficient angular 'narrowness' of the directional pattern. At close distances (actually, within the limits of $\lambda < r \leq (D^2/n\lambda)$, where $n > 10$–$20$ is an integer) the synphase property of the front is not yet violated, and the wave behaves as if it were almost planar. This is the geometric optics zone, or the so-called searchlight ray zone, in which virtually the whole power emitted by an antenna is concentrated. Then, in the range of distances $r \cong D^2/n\lambda$ $(10 > n > 1)$ the synphase property is essentially violated, which is accompanied by strong oscillations of the field amplitudes (and,

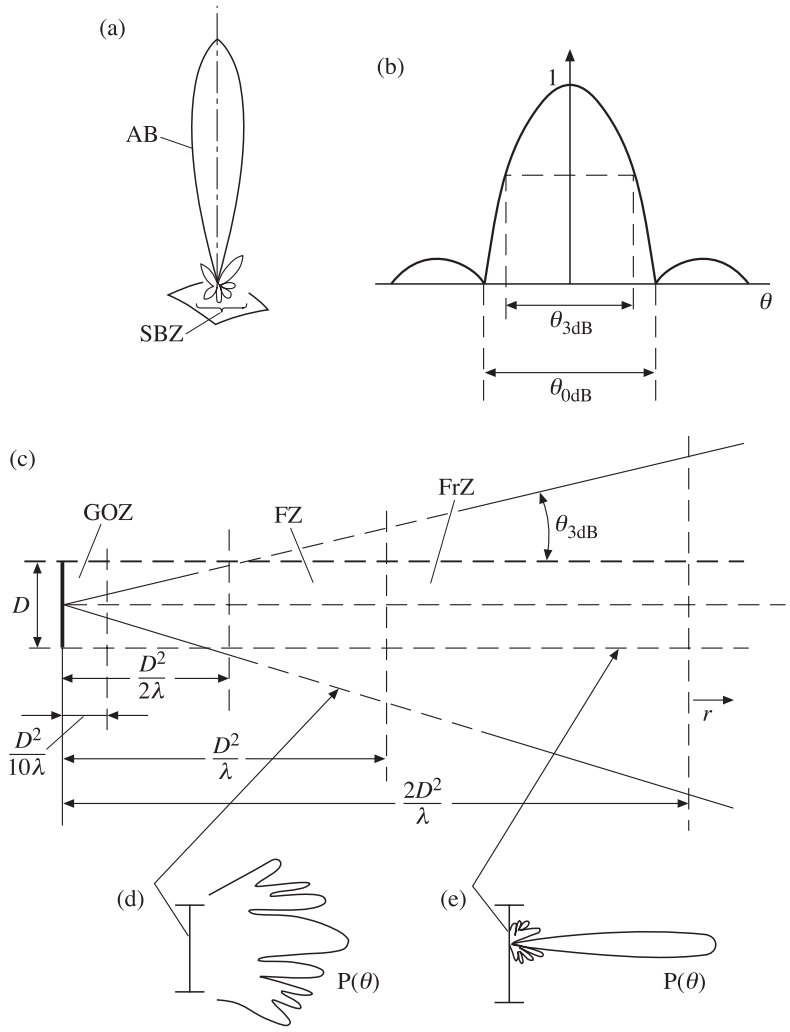


**Figure 5.3.** Schematic presentation of an antenna directional pattern (ADP) formation. (a) ADP is in plane polar coordinates. AB is an antenna (main) beam; SBZ is side beam zone. (b) ADP section is in Cartesian coordinates. (c) Special evolution of emergent wave beam. GOZ is geometrical optics zone; FZ is Fresnel zone (pulsed beam zone); FrZ is Fraunhofer zone (far zone). (d) ADP in Fresnel zone. (e) ADP in Fraunhofer zone.

accordingly, of Poynting's vector), in the direction of propagation as well. This is the Fresnel diffraction zone. And, finally, for $r \gg D^2/\lambda$ (or, as conventionally accepted, for $r > 2D^2/\lambda$) the wave front becomes spherical, the field decreases as $1/r$ (and, accordingly, the Poynting's vector magnitude as $1/r^2$), and the oscillations of amplitudes in the direction of propagation actually disappear. This is the far zone of an antenna (or the Fraunhofer zone), where it is already possible to operate with the

notion of directional pattern, i.e. with the dependence of the field amplitude on the angular coordinates only.

The question of the relation between the power of the signal received by the main and side lobes (or, in other words, the question of the antenna system efficiency) is so important for microwave systems (for a number of reasons) that we shall consider it in a separate section.

Note, once again, one of important corollaries of the reciprocity theorem, namely, the full coincidence of directional patterns of an antenna in its operation both in reception and in emission modes.

### 5.2.3 The effective surface

For receiving antennas, along with their angular characteristics, the parameters determining the total power of a received signal are of importance. According to the definition of antenna directional pattern (ADP) as a characteristic of the antenna which performs reception of a planar electromagnetic wave intensity from a given direction, and taking into account (5.2) and (5.8), we can write a power signal received by an antenna from the external source as

$$W_\nu \, \mathrm{d}\nu = \tfrac{1}{2} A \, \mathrm{d}\nu \iint_{4\pi} I_\nu(\theta, \varphi) P(\theta, \varphi) \, \mathrm{d}\varphi \sin\theta \, \mathrm{d}\theta, \tag{5.15}$$

where coefficient $A$ characterizes the degree of efficiency of an antenna as an instrument designed for the reception of a received signal's power. This parameter is called the effective area (surface) of an antenna system (its dimension is $\mathrm{m}^2$).

Thus, expression (5.15) represents the power of the monochromatic flux received by an antenna from the external radiation throughout its physical surface per unit frequency band. It should be noted here that the external radiation falls on the antenna system from all directions within the limits of a spherical solid angle.

If the whole power falling on the antenna aperture were to be absorbed by it, then the effective surface would be equal to the geometric area of its aperture. Since, however, some part of the power is scattered by structure elements, and another part is lost in Joule's (resistance) losses, the effective surface of a real antenna will always be lower than the geometrical surface of an aperture.

If we consider the planar surface, then, in accordance with (5.2), by the generalized response to a planar electromagnetic wave of such a simple structure (some kind of ADP) can be meant the quantity $P(\theta) = \cos\theta$. Of course, such a structure is not used as a real antenna.

If, for an incident external radiation, $I(\theta, \varphi) = \text{const}$, or, in other words, the question is about the wide-angle (relative to ADP) source, then in this case (5.15) is transformed to the following form:

$$W_\nu \, \mathrm{d}\nu = \tfrac{1}{2} A \, \mathrm{d}\nu I_\nu \Omega_\mathrm{A}, \tag{5.16}$$

where by $\Omega_\mathrm{A}$ is meant the quantity called the total antenna-pattern solid angle:

$$\Omega_\mathrm{A} = \iint_{4\pi} P(\theta, \varphi) \, \mathrm{d}\Omega. \tag{5.17}$$

It is not difficult now to find the relation of this characteristic to the plane angular characteristics. Suppose (for clarity), that the ADP represents a symmetric spherical cone with the plane angular aperture $\theta_{0.5}$ and $P(\theta, \varphi) = 1$. Using the well-known definition of a solid angle as the ratio of the area of a sphere, limited by this angle, to the square of the radius of a sphere, we have

$$\Omega = \frac{S(\theta)}{R^2} = 2\pi(1 - \cos\theta). \tag{5.18}$$

Considering the small plane angles only (the beam antennae), we shall have, after some transformations:

$$\Omega_{\mathrm{A}} = \frac{\pi}{4}\theta_{3\mathrm{dB}}^2. \tag{5.19}$$

This relation gives rise to the name of solid angles as square degrees, which is often used in observational practice. We should have in mind here, that one steradian contains 3282 square degrees (see Appendix A).

If, however, a very compact source (in relation to the ADP angular size) is observed, then it can easily be seen that relation (5.15) can be reduced to the following form (if the source is directed strictly to the main lobe):

$$W_\nu \, \mathrm{d}\nu = \tfrac{1}{2} A \, \mathrm{d}\nu I_{\mathrm{S}} \, \Omega_{\mathrm{S}} \tag{5.20}$$

Here $I_{\mathrm{S}}$ and $\Omega_{\mathrm{S}}$ are the intensity and angular size (a solid angle) of a compact source.

### 5.2.4 Antenna directivity

This numerical (dimensionless) parameter ($D$) means the quantity, which indicates to what extent the directional properties of the given antenna differ from an ideal spherical emitter, i.e. an emitter whose directional pattern in power equals unity regardless of spherical coordinates. Thus, the antenna directivity is equal to:

$$D = \frac{4\pi}{\Omega_{\mathrm{A}}}. \tag{5.21}$$

For beam antennas this quantity can be equal to tens or hundreds of thousands of units.

### 5.2.5 Antenna gain

This numerical parameter $G(\theta, \varphi)$ means the product of an antenna directivity and its normalized ADP in power, i.e.

$$G(\theta, \varphi) = DP(\theta, \varphi). \tag{5.22}$$

It is clear from physical considerations that the antenna parameters considered above (the effective area, solid angle and antenna directivity) are closely interrelated. So antenna theory (see, for example, Tseitlin, 1966) rigorously indicates that the following relation takes place:

$$A\Omega_{\mathrm{A}} = \lambda^2, \tag{5.23}$$

where $\lambda$ is the working wavelength. It follows from this relation, that the antenna directivity is related to its effective area as:

$$D = \{4\pi/\lambda^2\}A. \tag{5.24}$$

We shall repeatedly use these relations hereafter.

The antenna systems characteristics listed above depend on the frequency, of course. The frequency range, in which the characteristics can be considered invariable, is called the antenna passband. In many cases, however, antenna systems can be built whose parameters insignificantly vary within a very wide frequency band, and, thus, the frequency limitations of the entire receiving system will be stipulated by input components of amplifying devices (see Chapter 3).

A huge band of wavelengths, emitted or received by antennas, and the diversity of fields of their application (communications, television, radar, remote sensing, radio-astronomy) gave rise to many types and configurations of antenna systems, described in a number of specialized publications.

The problems of designing antennas with specified characteristics for the appropriate field of application constitute the subject of special research and design work. And here for various fields of application (such as radio communication, radar, microwave sensing) quite specific requirements should be satisfied which may not be so significant for other applications. Below we shall consider the basic requirements of antenna systems designed for microwave sensing.

## 5.3 ANTENNAS AND BRIGHTNESS TEMPERATURES

Before formulating the basic requirements for antenna systems for microwave sensing we shall consider in more detail the important problem (we have already considered briefly before) of the determination of and relationship between antennas and brightness temperatures in microwave sensing.

One of the important parameters characterizing the power of a signal received by an antenna and transmitted directly to a receiving device is the antenna temperature. This definition is introduced proceeding from the following equivalent scheme of measurements (Figure 5.4). A portion of the electromagnetic energy of a source, released by the solid angle of ADP, passes through the antenna system, being transformed into the mode of the electromagnetic wave propagating in the transmission line. The conditions of transformation of received electromagnetic signal energy, which include also the transformation of modes of oscillations, are specially selected in such a manner that the maximum power of the signal, received by an antenna, be transmitted into a receiving device. The design features of this transformation in a particular antenna and in the antenna transmission line can be very complicated. For the purposes of the physical understanding of this process, investigators resort to the equivalent schemes (see section 3.3). The whole process of signal reception and transformation by an antenna system is represented in the form of the emf source and active resistance ($R_A$), which is some kind of equivalence of the antenna and is placed in the thermostat with physical temperature

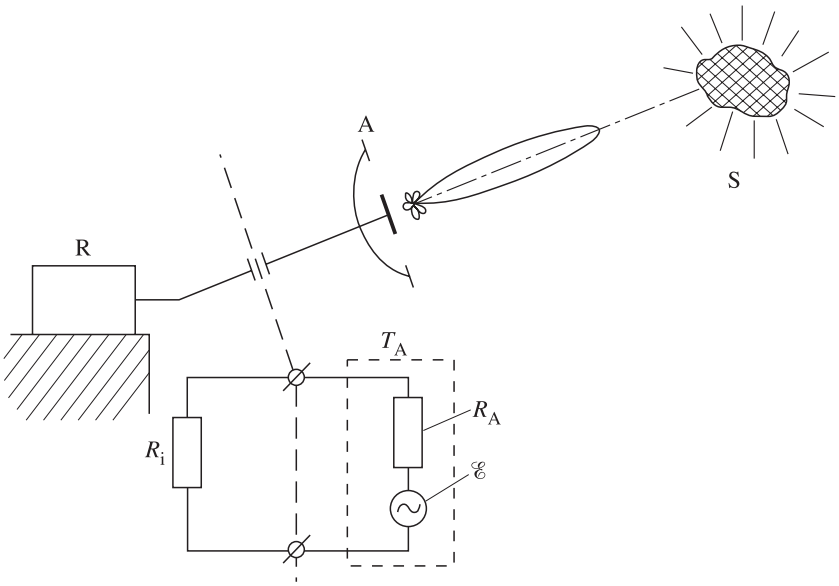


**Figure 5.4.** Schematic presentation of receiving procedure for the antenna temperature determination. S is a source; A is antenna; R is a radiometer. $T_A$ is a thermostat temperature (antenna temperature); E is effective emf.

$T_A$. The amplifying device is presented in the form of input active resistance ($R_i$) (Figure 5.4). As we have already seen (see section 3.3), the maximum transmission of power from an antenna system into an amplifying device is possible only under the condition of coordination, i.e. with the equality $R_A = R_i$. Under this condition the whole of the power received by an antenna in the frequency band unit, $W_\nu \, d\nu$, hits directly into a receiving device and, in accordance with (3.4), we can write

$$W_\nu \, d\nu = kT_A \, d\nu. \tag{5.25}$$

By $W_\nu$ here, in essence, is meant the spectral density of a signal received by an antenna from an external source (see equation (3.5)).

Thus, the antenna temperature $T_A$ (reduced to the frequency band unit) can be determined (and measured) as the physical temperature of the conventional thermostat with a coordinated resistance, in which, owing to thermal motion (the fluctuations), the fluctuation power is released, which is equal to the power of a fluctuation signal received by an antenna system. It is important to note that, according to the definition introduced above, the antenna temperature is reduced to the frequency band and, accordingly, it is proportional to the spectral density of a signal received by an antenna.

In order to find the relation between the antenna temperature and emission properties of a source, we shall write the expression for the power, transformed by an antenna, in another form, namely, from the viewpoint of the amount of

a signal's energy received by an antenna from free space. Recalling expression (5.15), we have:

$$W_\nu \, d\nu = \tfrac{1}{2} A \, d\nu \iint_{4\pi} I_\nu(\theta, \varphi, \nu) P(\theta, \varphi) \, d\Omega. \tag{5.26}$$

Further on, not considering the physical nature of an external source, we shall use (still in a formal manner) for the source intensity the expression that follows from the Rayleigh–Jeans law (see Chapter 6 for more details), namely:

$$I_\nu(\theta, \varphi, \nu) = \frac{2k}{\lambda^2} T_B(\theta, \varphi, \nu). \tag{5.27}$$

Here by $T_B(\theta, \varphi)$ we shall mean the brightness temperature of a source (or of the surface of an emitting medium). Note, that, according to the definition introduced above, the brightness temperature of a source itself (as well as the antenna temperature of the same source) is reduced to the frequency band unit and, accordingly, it is proportional to the spectral density of the fluctuation signal of a source (see equation (3.5)). Note once again that the introduced definition of brightness temperature is in no way related to radiation physics. It is equally used both for physical objects with thermal emission (such as the terrestrial surface) and for objects with a non-thermal character of emission (such as the artificial sources of pseudo-noise emission in radar, the radio-emission of the ionosphere and magnetosphere, and the astrophysical objects of maser radiation).

Substituting expressions (5.23), (5.25) and (5.27) into (5.26) and making some simple transformations, we obtain the following important relation for the antenna temperature expression:

$$T_A(\nu) = \frac{\iint_{4\pi} T_B(\theta, \varphi, \nu) P(\theta, \varphi) \, d\Omega}{\iint_{4\pi} P(\theta, \varphi) \, d\Omega}. \tag{5.28}$$

Since the antenna temperature is proportional to the spectral density of a signal, the total power of a signal ($W$), received by the antenna system and reduced to the amplifying system input, will be equal to:

$$W = k \frac{1}{\frac{1}{\Delta\nu} \int_{\Delta\nu} G(\nu) \, d\nu} \int_{\Delta\nu} G(\nu) T_A(\nu) \, d\nu, \tag{5.29}$$

where $G(\nu)$ is the amplitude-frequency characteristic (in power) of the receiving amplifier. If the antenna temperature does not change within the limits of the amplifier passband, then expression (5.29) is simplified up to the form, which is often used in practical estimation calculations:

$$W = k T_A \, \Delta\nu = k T_A \, \Delta f, \tag{5.30}$$

where $\Delta\nu = \Delta f$ is the power passband of the amplifier unit (see section 3.8).

Let us return to analysing the expression for the antenna temperature (5.28). It can easily be seen, that, depending on the relation between the effective angular size

of a source and antenna and on the source intensity value, the antenna temperature value can vary within wide limits. Consider now two extreme cases: the first, where the angular size of a source is essentially larger than the angular size of ADP (the so-called extended source), and the second, where the angular size of a source is essentially smaller than the angular characteristics of ADP (the so-called discrete source, or 'hot spots').

### 5.3.1 Extended source

The extended source includes, for example, emitting surfaces of Earth surface type (sea surface, land) as observed from low-orbit spacecraft and from aircraft, as well as the detailed investigations of emission of the surface of the Sun, Moon and planets by means of beam antenna systems. Since for this type of source its angular size $\Omega_S \gg \Omega_A$, $T_B$ can be considered to be a constant value within the limits of the angular size of ADP and can be brought outside the integration sign. In this case (5.28) acquires the following form:

$$T_A(\theta, \varphi) = T_B(\theta, \varphi). \tag{5.31}$$

At first sight, the expression obtained for the antenna temperature is paradoxical, since the received power from a source does not depend on the distance to a source and on antenna system parameters. However, this paradox is only apparent since, as the distance $r$ (the height over the studied surface) increases, under beam antenna conditions and within the limits of angular resolution of ADP the emitting area increases as $r^2$, whereas the Poynting vector magnitude decreases as $r^{-2}$, and, thus, the total power, collected from the ADP-illuminated area (or instantaneous field of view), remains unchanged.

### 5.3.2 Discrete source

The discrete source includes such sharp and intensive inhomogeneities on the terrestrial surface as forest fires, erupting volcanoes, and breaking sea waves, as well as numerous remote radio-astronomical objects (quasars, pulsars, radio galaxies, maser sources).

Since for this type of source its angular size $\Omega_S \ll \Omega_A$, quantity $P(\theta, \varphi)$ can be considered to be constant and equal to unity within the limits of angular sizes of a source. This allows us to apply the theorem of the average to the upper integral. In this case the expression for antenna temperature is transformed as follows:

$$T_A = \frac{\iint_{4\pi} T_B \, d\Omega}{\iint_{4\pi} P \, d\Omega} = T_{BS} \frac{\iint_{4\pi} d\Omega}{\iint_{4\pi} P \, d\Omega} = T_{BS} \frac{\Omega_S}{\Omega_A}, \tag{5.32}$$

where $T_{BS}$ and $\Omega_S$ are the averaged values of intensity of a source (within the limits of its solid size) and its angular size.

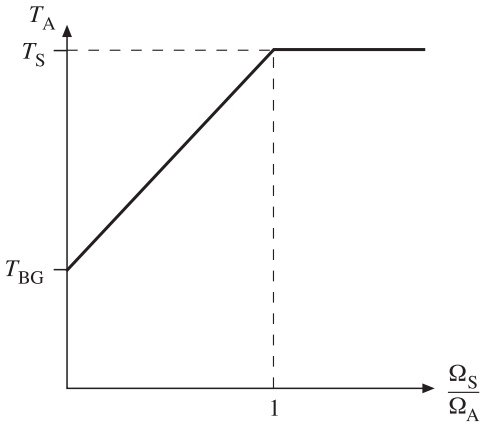


**Figure 5.5.** The relationship of antenna temperature value to a solid angular value of source. $T_{BG}$ and $T_S$ are brightness temperatures of thermal background and of a 'warm' source (see equation (5.33)).

It can easily be seen that the expression obtained critically differs from the expression for an extended source. The antenna temperature value depends both on the distance to a source (in terms of the value of its solid angle size), on its intensity, and on the antenna system parameters.

Using these two extreme cases, we can easily write the expression for antenna temperature of a bright discrete source with intensity $T_S$ with solid angular size $\Omega_S$ against the extended thermal background $T_{BG}$:

$$T_A = T_S \frac{\Omega_S}{\Omega_A} + T_{BG}\left(1 - \frac{\Omega_S}{\Omega_A}\right). \tag{5.33}$$

Figure 5.5 presents the dependence of antenna temperature on the angular (in a solid angle measurement) size of a 'hot' source against the 'cold' background ($T_S > T_{BG}$). Note that, as the source area increases, its contribution to the total temperature (or, as is sometimes said, the radio contrast) increases linearly and, when reaching the size of the ADP field of view area, reaches a maximum. Certainly, the opposite situation is also possible, namely, the 'cold' source against the 'warm' background. A typical example of such a situation is the presence of an opening in ice – the so-called polynya (the 'cold' source) in a marine ice sheet (the 'warm' background) (see Chapter 8).

To describe the discrete sources which cannot be resolved in detail for some reason or other, the notion of the magnitude of energy flux from a source is introduced into radio-astronomy. In some cases this definition has started to be used in microwave sensing as well. The spectral source flux implies the following quantity:

$$F_\nu = \iint_{4\pi} I_\nu(\theta, \varphi, \nu) P(\theta, \varphi)\, \mathrm{d}\Omega. \tag{5.34}$$

**Table 5.1.** The main characteristics of radiotelescopes (the Crimea, Pushchino)

| Radiotelescope location | Antenna diameter, m | Antenna beamwidth, plane angular minute | Effective surface, $m^2$ | Noise temperature, K | Flux sensitivity, Jy |
|---|---|---|---|---|---|
| Simeis (the Crimea) | 22 | 2.5 | 150 | 80 | 0.4 |
| Eupatoria (the Crimea) | 70 | 0.7 | 1500 | 60 | 0.03 |
| Pushchino (Moscow region) | 22 | 2.5 | 110 | 120 | 0.8 |

Using the expression for the Rayleigh–Jeans law, the theorem of the average, and taking into account the small angular size of a source, we can rewrite (5.34) in the form:

$$F_\nu = \frac{2k}{\lambda^2}\iint_{4\pi} T_B \, d\Omega = \frac{2k}{\lambda^2} T_{BS}\Omega_S. \tag{5.35}$$

Thus, the antenna temperature from a discrete source can be presented in three equivalent forms:

$$T_A = T_{BS}\frac{\Omega_S}{\Omega_A} = \frac{1}{2k}AF_\nu = \frac{A}{\lambda^2}T_{BS}\Omega_S. \tag{5.36}$$

It follows from this condition, that the sensitivity of the radiothermal complex can be defined both as the sensitivity in antenna temperature, and as the sensitivity in minimally detectable fluxes from pointwise (discrete) objects of investigation. As we have already noted, in radio-astronomy the flux unit, or jansky (Jy), is accepted as the flux measurement unit and the 3C 273 quasar radio-emission source with a radiation flux of 30 Jy is often used for estimations in calibration work. As an example, we refer to the operational data and flux sensitivity data for a series of Russian radio telescopes (Table 5.1) (Matveenko *et al.*, 1983), the information on which is not widespread in Western literature.

## 5.4 THE SCATTERING COEFFICIENT OF ANTENNAS

The principal feature of radiothermal observations (unlike radio communication or reception of radio broadcasting and television programmes) consists in the fact that the statistical properties of a signal, received at the main lobe (the 'useful' signal, conventionally) and at side lobes (the 'parasitic' signal), are identical (Gaussian noise). Also of importance is the fact that the contribution of these components is

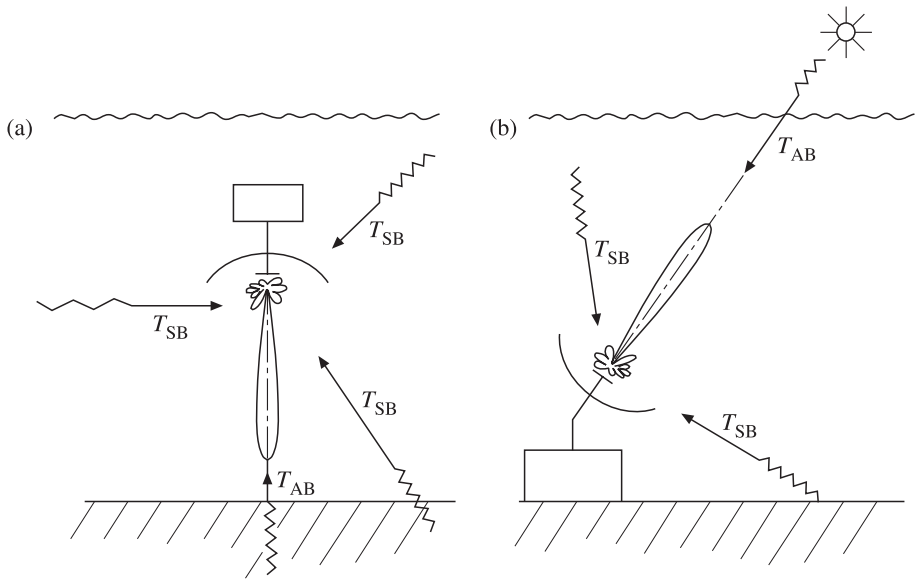


**Figure 5.6.** Schematic presentation of the antenna temperature components. (a). Airborne radiometric variant of observations. (b). Radio-astronomical variant of observations.

comparable in intensity. Thus, the recognition and detection of these components from purely statistical tests is impossible. Moreover, in a series of cases the useful signal (or its spatial-temporal variation) constitutes a value essentially lower than the noise radiation contribution into the side-lobe field of ADP. The problem of maximally reducing the contribution of side-lobe radiation to the total signal is of major importance, both for radio-astronomy (Esepkina *et al.*, 1973) and for microwave sensing.

Figure 5.6 shows the onboard radiothermal instruments installed on the flight vehicle in the Earth's atmosphere, and the main components of a received noise signal. The total noise signal can be separated into three groups: the noise signal received at the main lobe (antenna beam), and the noise signals received in the side-lobe (side-beam) zone. The latter signals will include the components received from the Earth's surface and from the atmosphere. Since all these components are statistically independent, their intensities (variances) are added (see section 2.2), and, thus, the expression for antenna temperature can be written as:

$$T_A = \frac{\iint_{4\pi} T_B P \, d\Omega}{\iint_{4\pi} P \, d\Omega} = \frac{\iint_{\Omega_{AB}} T_B P \, d\Omega}{\iint_{4\pi} P \, d\Omega} + \frac{\iint_{\Omega_{SB}} T_B P \, d\Omega}{\iint_{4\pi} P \, d\Omega}. \tag{5.37}$$

Now we introduce the following important definition: the coefficient, which characterizes the portion of energy, emitted (or absorbed) by an antenna into the

side-lobe zone, will be called a scattering coefficient and will be defined in accordance with the following relation:

$$\beta = \frac{1}{\iint_{4\pi} P\,\mathrm{d}\Omega} \iint_{\Omega_{SB}} P\,\mathrm{d}\Omega. \tag{5.38}$$

The averaged temperatures of radiation over solid angles of the main lobe and over the remaining space are written as:

$$T_{AB} = \frac{\iint_{\Omega_{AB}} TP\,\mathrm{d}\Omega}{\iint_{\Omega_{AB}} P\,\mathrm{d}\Omega}; T_{SB} = \frac{\iint_{\Omega_{SB}} TP\,\mathrm{d}\Omega}{\iint_{\Omega_{SB}} P\,\mathrm{d}\Omega}. \tag{5.39}$$

In such a case, expression (5.37) can easily be rewritten in the following form, which is often used in observational practice:

$$T_A = T_{AB}(1-\beta) + T_{SB}\beta. \tag{5.40}$$

The total signal, received by an onboard radiothermal complex, will consist of the components received by an instrument in quite different directions (from various solid angles), but (we emphasize once again) completely indiscernible statistically. In the majority of cases it is expedient to separate the $T_{SB}$ component into a component determined over the lower hemisphere and a component determined over the upper hemisphere. Whereas in the lower hemisphere the emission emanates from the Earth's surface, in the upper hemisphere the emission is determined by emission from the atmosphere and outer space (the 'relic' background and radio sources) (Figure 5.6).

As an instructive example, we shall consider the problem of a scattering coefficient of the model antenna composed of two cones: the main lobe (with ADP equal to unity) and the side-lobe zone with ADP equal to $P_1 = -40$ dB. This level of side emission is considered as quite good. To calculate the scattering coefficient value we perform the following transformations:

$$1-\beta = \frac{\iint_{4\pi} P\,\mathrm{d}\Omega - \iint_{\Omega_{SB}} P\,\mathrm{d}\Omega}{\iint_{4\pi} P\,\mathrm{d}\Omega} = \frac{\iint_{\Omega_{AB}} P\,\mathrm{d}\Omega}{\iint_{\Omega_{AB}} P\,\mathrm{d}\Omega + \iint_{\Omega_{SB}} P\,\mathrm{d}\Omega} = \frac{1}{1 + P_1 \dfrac{\Omega_{SB}}{\Omega_{AB}}}. \tag{5.41}$$

Since the question is now about the antenna with high resolution, the solid angle of a side-lobe zone can be replaced, with good approximation, by the total solid angle of $4\pi$. And then, recalling expression (5.21), we shall write the scattering coefficient in terms of the value of directivity as:

$$1-\beta = \frac{1}{1+P_1 G}. \tag{5.42}$$

Suppose the antenna directivity to be $G = 1000$. In this case the solid angle of an antenna will be 0.012 steradians and, accordingly, its value in square degrees will be equal to 39.3. In the linear dimension, however, the ADP will be 6.2 angular degrees. Antennas with such angular characteristics are often used in microwave practice (see Chapter 14). Substituting the values of antenna directivity and side-lobe level into (5.42), we obtain the value of the scattering coefficient of an antenna to be 0.09 (or 9%). We pay attention to the fact that, although the side emission level is very low, the energy escaping to side emission is significant. Certainly, this is a consequence of the large solid angle zone of side lobes.

We can easily see the reasons why the emission contribution to the side-lobe zone may be critical for carrying out an observational experiment. Suppose, that we use the aforementioned antenna (as the 'ground-based' radio telescope, Figure 5.6(b)) for studying the radio-emission of the Moon (the brightness temperature is 250 K and the angular size is 0.5°). Using formula (5.32), we obtain the value of antenna temperature at the main lobe as

$$T_{AB} = 250 \left(\frac{0.5}{6.2}\right)^2 = 1.6\,\text{K}. \tag{5.43}$$

The space surrounding an antenna (the Earth surface and atmosphere) has (on the average) a brightness temperature value of about 270 K. Thus, the total antenna temperature of an antenna will be:

$$T_A = 1.45 + 24.3 = 25.75\,\text{K}. \tag{5.44}$$

It follows from this fact, that 94% of a signal received by an antenna constitutes a 'parasitic' signal. Changing the position angle of the main lobe of an antenna (in the guidance or tracking mode) will also change this parasitic signal – in a virtually uncontrollable manner. This model example clearly demonstrates the major problem of ground radio telescopes: the necessity of maximally reducing the powerful parasitic signal from the ground objects and atmosphere (Esepkina *et al.*, 1973).

Referring to the study of extended and fairly homogeneous objects (such as the sea surface) (Figure 5.6(a)), the situation seems to be essentially simplified here, since the expression (5.40) can be rewritten as follows:

$$T_A = T_{AB} - (T_{AB} - T_{SB})\beta. \tag{5.45}$$

Detailed onboard experiments under full-scale conditions have shown (Veselov *et al.*, 1981) that the difference between the temperatures measured at the main lobe and at the side-lobe zone is quite small (of the order of 20–30 K). In such a case, using the aforementioned model example for the situation with an extended source (Figure 5.6(a)) (with the brightness temperature of 200 K), we have the value of the total antenna temperature in the form

$$T_A = 200 - 30 \times 0.09 = 197.3\,\text{K}. \tag{5.46}$$

It can be seen from this expression that the possible relative error is (at first sight) fairly insignificant (about 1.5%). However, those addressing the physical problems

of studying the World Ocean surface much higher requirements, namely, the measurement of brightness contrasts (at the main lobe) at the level of 0.1–5 K. Thus, in formulating such problems the possible radiothermal variations of the same order, which arise from radiothermal surface contrasts in the side-lobe zone (and which, accordingly, cannot be controlled on the solid angle zone of $2\pi$), can already be considered inadmissible – the more so as at installation on a flight vehicle the side-lobe zone (but, we note, not the shape and angular size of the main lobe) can essentially be distorted because of design features of attaching the antenna system to the vehicle. The appropriate experimental methodology on detailed measurement of onboard antenna systems and on performing calibration procedures has now been developed (see section 5.8).

In concluding this section we note that similar problems do not arise with the reception of television and radio broadcasting programmes and in radio communications, though the scattering coefficient of television antennas can reach 50–70%. This is due to the fact that the useful signal, received at the main lobe, exceeds by a factor of $10^7$–$10^9$ (on the average), the signal received by a receiver from an ambient medium in the side-lobe zone; and, thus, the 'parasitic' signal is not distinguishable against the useful signal. However, in the case of detailed radar and scatterometric measurements, where an ouput powerful signal is emitted, the problem of reducing the reception of 'parasitic' backscattering in the side-lobe zone is also topical. However, in virtue of the specificity of active measurements, the methodology used in this case differs from that used in passive radiothermal measurements.

## 5.5 ANTENNA TEMPERATURE OF ANTENNA WITH RESISTANCE LOSS

The above considerations have related to ideal (lossless) antenna systems, i.e. to receiving systems not possessing intrinsic resistance losses at reception and transmission of a signal. However, real antenna systems and antenna transmission lines (ATL), which connect the antenna itself and a receiving device, possess determinate (and unremovable) resistance losses and, accordingly, intrinsic fluctuation emission (see Chapter 4). In radiothermal observations (unlike radio communications or reception of broadcast radio and television programmes) the statistical properties of signals, received by an antenna and arising in the antenna and antenna transmission lines, are identical (the Gaussian noise), and, certainly, they cannot be distinguished by means of purely statistical procedures. Besides, if the radiothermal measurements are carried out by means of a receiving system that is conditional on strong (and not constant) temperature gradients (as, for example, in the case of an instrument installed onboard a spacecraft without a thermal control system), then the values of 'parasitic' signals can be comparable to, and even exceed, 'useful' values.

There exists, certainly, a fairly complete theory of calculating the losses in antenna systems and intrinsic radiation. Here, however, we shall make use of

physical considerations for estimating the contribution of resistance losses to the emission properties of antennas. Suppose that an antenna system with the power transmission coefficient $\eta$ and the receiving device itself are immersed in thermostat conditions with temperature $T_0$. The antenna temperature, received by a receiving device, will consist of two statistically independent components: the external signal $\eta T_{A0}$, received directly by an antenna and partially decreased due to resistance losses, and signal $T_{ATL}$, which arises directly in the antenna transmission line. Since these signals are statistically independent, their intensities (variances) can be added. In this case the total signal at the receiver input will be as follows:

$$T_A = T_{A0}\eta + T_{ATL}. \tag{5.47}$$

Since the whole system is situated inside the thermostat, the full equilibrium conditions should be satisfied. In other words, the signal, which directly hits the antenna aperture, is equal to $T_0$, and the total signal recorded by a receiver should also be equal to $T_0$. Substituting the values mentioned into expression (5.47) and performing very simple manipulations, we obtain the value of brightness temperature of the fluctuation signal caused by resistance losses in a line:

$$T_{ATL} = T_0(1 - \eta). \tag{5.48}$$

This expression is widely used in the practice of microwave remote sensing and radio-astronomical observations. We shall also use this relation repeatedly below. From the viewpoint of thermal radiation physics, the relation obtained is nothing other than the Kirchhoff law in an unusual form.

Thus, the total signal, reaching the amplifier's input after passage through the antenna transmission line, can be written as:

$$T_A = T_{A0}\eta + T_0(1 - \eta). \tag{5.49}$$

We emphasize, that by $T_0$ here is meant the thermodynamic temperature of an antenna and antenna transmission line. This directly stipulates the importance of the problem of the thermal stabilization of an antenna transmission line. So, if for any physical reason it is necessary to perform radiothermal measurements to an accuracy of $\Delta T$, then the thermal stabilization of an antenna transmission line should be better, than $\Delta T/1 - \eta$, throughout the course of the experiment. For example, for an antenna system with $\eta = 0.9$ and for a measurement accuracy of 0.1 K the thermal stabilization of an antenna and antenna transmission line should be better than 1 K. Such a design problem in itself and the temporal stability of these parameters can be quite complicated in the case of an antenna system installated on a space vehicle (Ruf, 2000a,b; Njoku *et al.*, 2000b; Keihm *et al.*, 2000; Colton and Poe, 1999).

The complete expression for the antenna temperature with regard to the contribution of a side emission (equation (5.40)) and intrinsic noises (equation (5.49)) can be written in the form

$$T_A = T_{AB}(1 - \beta)\eta + T_{SB}\beta\eta + T_0(1 - \eta). \tag{5.50}$$

Making use of the model examples from the previous paragraph, we shall estimate the contribution from side emission and from intrinsic noises into the total signal. For the example of radio-astronomical observations, taking account of the 'true' signal value as 1.6 K, the brightness temperature in the side-lobe zone as 270 K, the values $\eta = 0.9$ and $\beta = 0.09$ and thermodynamic temperature of an antenna as 300 K, we obtain the following value for a total signal:

$$T_A = 1.3 + 21.87 + 30 = 53.17\,\text{K}. \tag{5.51}$$

It follows from this result that more than 97% of signal intensity relates to the 'parasitic' signal. Thus, one of the most important design problems in the development of radio telescopes is to ensure minimum losses at signal transmission from an antenna to a receiving device (Tseitlin, 1966; Esepkina *et al.*, 1973; Wilson and Huttemeister, 2000; Poperechenko, 2000; Peng and Nan, 2002).

In the case of onboard observations, taking into account the same values of the parameters, we shall have the value for a total signal as:

$$T_A = 197.3 \times 0.9 + 30 = 207.6\,\text{K}. \tag{5.52}$$

Unlike the previous case (equation (5.46)), we have now some kind of over-compensation (due to intrinsic noises) of a received signal, that is to say, the value of a received signal is greater than the value of a 'true' signal (200 K). As in the case of radio-astronomical observations, in designing radiothermal onboard complexes great attention is paid to minimization of losses in ATL. And so the designers try to manage, if at all possible, without including ATL components into the structure, by connecting the antenna directly to a receiving device (Amirkhanyn *et al.*, 1978; Strukov and Skulachev, 1984, 1986).

These model examples clearly indicate the importance of carefully accounting for the contribution of side lobes' emission and intrinsic antenna emission into the total signal and for the further procedure of restoring the 'true' signal. In actual observational practice the situation can, of course, be even more complicated than the model examples considered above.

Problems like those considered above virtually do not arise with reception of broadcast television and radio programmes and with radio communications. This is explained by the fact that the useful signal exceeds the signal which arises in the antenna transmission line by an order of magnitude on the average. Thus, the 'parasitic' signal is not distinguishable against the useful signal background (like in the case of radiation reception at side lobes).

## 5.6 SPATIAL-TEMPORAL DYNAMICS IN PASSIVE REMOTE SENSING

The previous analysis has related to the time-independent regime of observation. Real radiothermal observations, however, include the time-dependent aspect; for example, the motion of a flight vehicle over the surface being studied and, accordingly, the finite time of observation of an object. As we have noted above (section 3.5), the peculiarity of passive remote sensing lies in the fact that the main system

parameters (threshold sensitivity, the observation time constant, the instantaneous field of view of an antenna) are rigidly interrelated. And, in this connection, the spatial-temporal dynamics of the measurement process itself imposes fairly strict limitations both on the time of observation of an object and on the possibility of its recognition against the background of the intrinsic noise of the instrument. Certainly, similar problems also arise in the other fields of application of radiophysical systems (radio communications, television); but in those areas the relationships between these parameters are, for a number of reasons, essentially less critical.

To understand these interrelations we shall consider the model example: a radiothermal complex with an ideal antenna ($\eta = 1.0$ and $\beta = 0$) having a conical-shaped ADP, installed on a moving (at altitude $H$) carrier. If during the motion the vehicle encounters a contrast source with brightness temperature $T_S$ and area $S$, then, in accordance with (5.33), we have the extreme value for antenna temperature in the form:

$$T_A = T_S \frac{S}{S_A} + T_{BG}\left(1 - \frac{S}{S_A}\right). \tag{5.53}$$

where $S_A = H^2\Omega_A$ is the instantaneous field of view (IFOV) illuminated by an antenna on a studied surface.

As an example, we shall estimate the antenna temperature value for a water ice opening (a 'cold' object with $T_S = 150\,\mathrm{K}$), occurring in a sea ice sheet (a 'warm' background with $T_{BG} = 270\,\mathrm{K}$). If the ice opening area is equal to a half of the area of the instantaneous field of view of an antenna, then the minimum value of antenna temperature will be 210 K. In this case the contrast with the surrounding background will be negative and equal to 60 K. Note, that it is quite difficult to restore the emission characteristics of an object from the contrast value only, without resorting to additional information about the object geometry.

Let us consider now the same situation in dynamics, i.e. with allowance for the vehicle motion and finite sensitivity of the radiometer. If by quantity $V$ we mean the velocity of motion of a carrier on which the instrument is installed, then the full time, $t$, of 'scanning' the contrast object in the antenna's field of view will be

$$t = \frac{D_A}{V} = \frac{\theta H}{V}, \tag{5.54}$$

where $D_A = \theta H$ is the diameter of the field of view for beam antennas.

Here we should remember, that the radiometric complexes receive and process a signal not instantaneously, but with the delay function of exponential type (see Chapter 3) with time constant $\tau$. Thus, the total signal at instrument's exit is set up after (4–5)$\tau$. Therefore, to obtain at the instrument's exit the 'total' signal from a contrast object, we must ensure the following inequality: $t > 10\tau$. It follows from this condition, that the orbital features of a vehicle and the antenna system characteristics impose strict limitations on the constant of an instrument, namely:

$$\tau < \frac{\theta H}{10V}. \tag{5.55}$$

Violation of this inequality will result in the situation where the contrast objects will not be completely (either in intensity or in their characteristic size) presented in the output signal of a radiometer.

On the other hand, the time constant appears in the expression for the fluctuation sensitivity of a radiometer (see section 3.5), i.e. in the expression for the sensitivity threshold. In this case, for reliable recognition against the background of intrinsic noise of the instrument the value of the signal from a contrast object should not be lower than $3\Delta T/\sqrt{\tau}$, where $\Delta T$ is the normalized fluctuation sensitivity threshold (see section 3.5). The value of signal $\Delta T_S$ from a contrast object in the form of a circle of diameter $D_S$ will be equal to

$$\Delta T_S = (T_S - T_{GB})\frac{\Omega_S}{\Omega_A} = (T_S - T_{GB})\frac{\pi D_S^2}{16H^2\theta^2} \tag{5.56}$$

and, taking into account the above considerations on the recognition of a signal from an object, we shall have the second inequality the instrument's constant should satisfy:

$$\frac{\Delta T}{\sqrt{\tau}} < (T_S - T_{GB})\frac{D_S^2}{16H^2\theta^2}. \tag{5.57}$$

It can easily be seen that, unlike inequality (5.55), inequality (5.57) has an opposite character, i.e. it limits the time constant value 'from below'. Combining (5.55) and (5.57), we obtain a useful interval of time constant values, the fulfilment of which will allow us to completely record a signal against the background of noise components of an instrument:

$$\left(\frac{\Delta T}{T_S - T_{GB}}\right)^2\left(\frac{4H\theta}{D_S}\right)^4 < \tau < \frac{\theta H}{10V}. \tag{5.58}$$

Consider now the numerical example: on the possibility of recognition of a 'cold' object – the ice opening – against the 'warm' background by means of a radiothermal instrument with a normalized sensitivity of 0.1 K and ADP equal to 2.8° (or 1/20 radians). The radiothermal system parameters are close to those existing now (see Chapter 14). We shall suppose the satellite orbit's altitude to be 600 km, and the diameter of the circular-shaped ice opening to be 1 km. Substituting these values into (5.58), we obtain the following result:

$$144 < \tau < 0.4. \tag{5.59}$$

It can easily be seen that the requirements presented in (5.59) are mutually exclusive, and, therefore, the total signal cannot be recorded under the conditions mentioned. If, however, the object has a diameter an order of magnitude greater, namely, 10 km, then the situation radically changes, and the inequality will have the following form:

$$0.014 < \tau < 0.4, \tag{5.60}$$

which can surely be satisfied with the time constant of 0.05 sec. Figure 5.7 schematically presents the record of an output signal of a radiometer in the case of its recording above the considered object at the instrument's time constant of 0.05 sec

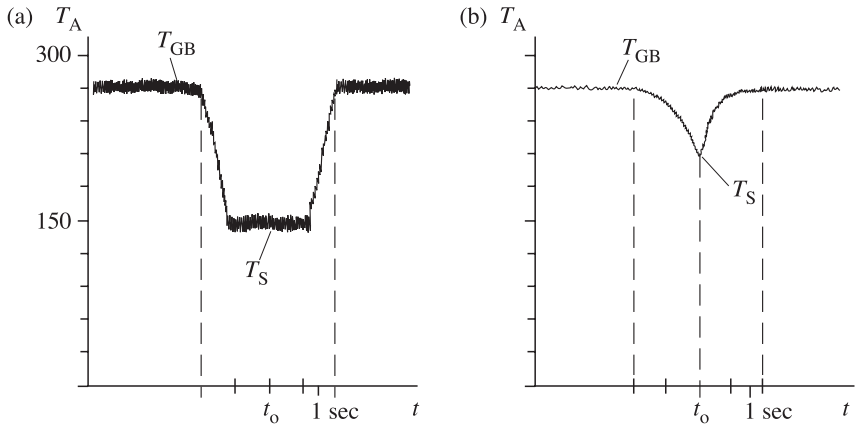


**Figure 5.7.** The signal registration at the moment ($t_0$) of the flight over a thermal 'cold' object. The integrator time parameter is (a) 0.05 s and (b) 1 s.

(Figure 5.7(a)) and at 1 sec. The principal distinctions between the two cases are clearly seen: in the first case the signal has completely recorded the object, whereas in the second case, in spite of the fact that the sensitivity of the system increased by nearly five times, the signal has obviously not been recorded completely. In this case the signal appears as though it consists of two 'torn off' exponents. This gives rise to the important and reliable experimental approach that would testify to complete signal recording: it is necessary to obtain, in the form of signal registration of such an object, either the 'plane bottom' (if the contrast is negative), or the 'plane cover' (if the contrast is positive).

## 5.7 THE EQUATION OF ANTENNA SMOOTHING

As we have already noted (see Chapter 1), the most important characteristic of an object is its spatial structure. However, in studying the spatial structure of objects in the microwave band investigators are in a much less favourable position (as compared to optics and the IR band) because of the greater length of the electromagnetic wave and, accordingly, the lower resolution capability. This circumstance has forced radio-astronomers to search for new methods of achieving high resolution that would allow them to 'synthesize' the image through the reception of a signal by several spaced radiotelescopes. And outstanding results have been obtained in this way, such as the fine structure of the region at the centre of our galaxy or the fine structure of distant quasars. In these works the resolution capability of synthesized radiotelescopes essentially exceeded the resolution capability which can be obtained by classical methods in optics. The theory and practice of image synthesis are based on the spatio-spectral methodology of generalization of properties of a radiotelescope as a filter of spatial frequencies.

The recently appearing spectrum of remote sensing problems requiring high spatial resolution in the microwave band put on the agenda the problem of synthesizing spatial fields by means of onboard radio interferometers taking into account the motion of a carrier (Milman, 1988; Ruf *et al*., 1988; Camps *et al*., 1997, 1998; Camps and Swift, 2000; Goutoule and de Boer, 2000; Dong *et al*., 2000). In spite of the obvious necessity of actively introducing spatio-spectral methodology into the theory and practice of microwave remote sensing, such ideas are not generally accepted yet in the microwave sensing. Nevertheless, we shall try to consider in this section the basic ideas of such an approach, which are mainly based on the experience of radio-astronomical observations (Esepkina *et al*., 1973).

The principal problem of onboard radiothermal satellite instruments is forming the radiobrightness field of an object under investigation. The radiobrightness distribution over the investigated surface, $T_{\mathrm{B}}(x, y, t)$, can be generally considered as a three-dimensional random function of spatial coordinates $(x, y)$ and time $(t)$ with a virtually unlimited detailed structure. As with any optical instrument (Born and Wolf, 1999), in microwave remote sensing the radiothermal satellite instruments play the part of a linear operator which influences the functions describing the object under investigation. The principal point in performing this operation (which is clear intuitively) consists in the fact that, in virtue of the limited angular resolution of an antenna, we shall essentially lose the details of any radio image obtained. A matter of principle here is whether we can restore the 'true' radio image, and, if so, how close it will be to the original. This very complicated problem is sometimes called the problem of 'superresolution'. But, before proceeding to analysis of the problem of restoring the true image, we shall consider the main principles of the spatio-spectral notions.

The fundamental formula, which will describe the procedure of the linear operator effect on spatio-energy characteristics of the investigated radiobrightness field can be obtained from the antenna temperature expression (5.28) with allowance for the vehicle motion over the investigated surface. In other words, the expression for ADP should be written in the moving Cartesian coordinate system $P(x - x'; y - y')$, where $x = V_x t$ and $y = V_y t$ (here $V_x$ and $V_y$ are the components of velocity of ADP motion along the corresponding coordinates). The integral that determines the value of the solid angle of an antenna (5.17) is in this case a constant quantity, and it is usually omitted in the basic formula. Transforming the antenna temperature expression from the polar coordinate system, fixed with the flight vehicle's antenna, into the system of Cartesian coordinates, fixed with the surface investigated, we obtain the following important relation called the equation of antenna smoothing:

$$T_{\mathrm{A}}(x, y) = \int_{-\infty}^{\infty} \int_{-\infty}^{\infty} T_{\mathrm{B}}(x'; y') P(x - x'; y - y')\, \mathrm{d}x'\, \mathrm{d}y', \tag{5.61}$$

where by $T_{\mathrm{B}}(x', y')$ is meant the 'true' radiobrightness field of an object. A thorough examination of relation (5.61) indicates, that it is none other than the

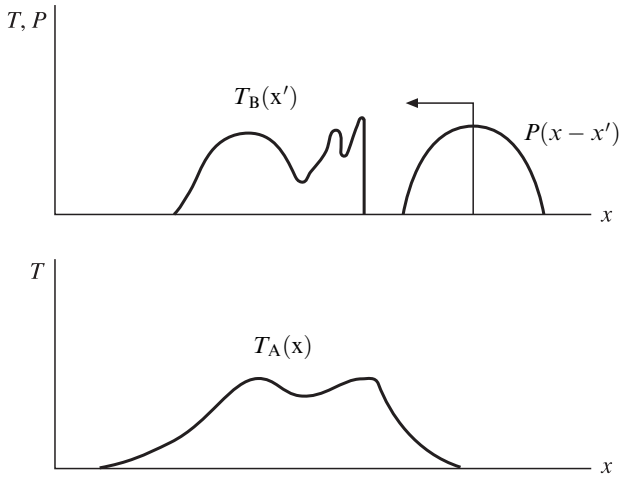


**Figure 5.8.** Schematic presentation of smoothing procedure for a complicated one-dimensional source $T_B(x')$ by antenna directional pattern (ADP) $P(x-x')$. $T_A(x)$ is the result of smoothing procedure.

convolution integral, which is usually written, with allowance for a commutative property, as:

$$T_A = T_B * P = P * T_B. \tag{5.62}$$

Generally speaking, the very fact that the observed field is a result of the convolution operation, testifies that the antenna system does not ensure obtaining the true result at observation, but yields some modified result. So, some kind of 'smoothing' of small details of the basic (or 'true') radio image takes place. For this reason the integral transformation of (5.61) was called the equation of antenna smoothing (Bracewell and Roberts, 1954). Figure 5.8 illustrates the sense of this transformation qualitatively. The instrument with the instantaneous field of view $P(x'-x)$ moves over the one-dimensional (for simplicity) radio object $T_B(x')$. As a result of smoothing, the instrument has recorded a signal which, generally speaking, essentially differs from the 'true' one, mainly by the absence of some fine (in scale, but not in physical significance) details. Certainly, if we imagine, that the ADP is infinitely narrow (as, for example, the delta-function), then in this case all details will be reproduced.

Let us show one more striking example of a smoothing procedure in the one-dimensional case for an object and ADP whose intensity and spatial form can be written as two plane sources (Figure 5.9). Substituting these values into (5.61), we obtain the result of convolution in the form:

$$T_A = \int_{-\infty}^{\infty} T_0(x')P_0(x-x')\,dx' = \frac{T_0P_0}{\Delta x}\begin{cases} x_0+\Delta x-x, & x>x_0 \\ -x_0+\Delta x-x, & x<x_0. \end{cases} \tag{5.63}$$

The important circumstance here is the fact, that the obtained signal has a basically different (in relation to an object) form; that is to say, it represents a triangle (rather

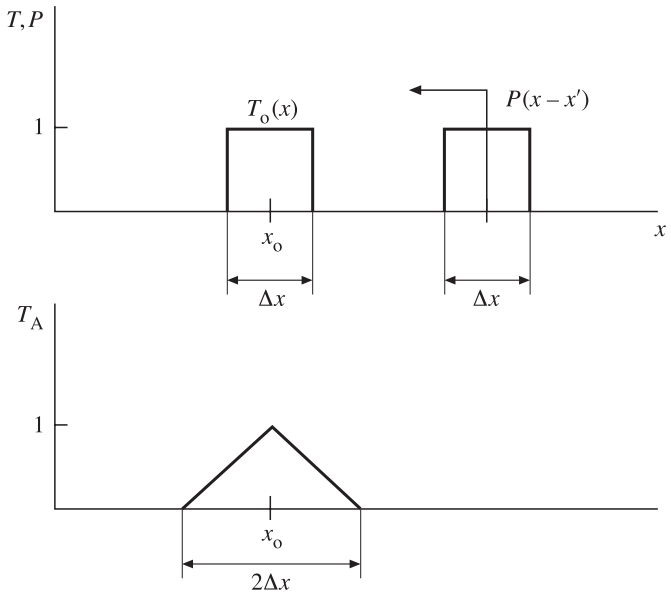


**Figure 5.9.** The smoothing procedure for two identical plane sources. $T_o(x)$ is a source $P(x - x')$ is ADP. $T_A(x)$ is the result of smoothing procedure.

than a rectangle). In this case its recorded size is twice as large as the original signal from the object. The analysis of the result of this simple model situation already demonstrates the difficulties the investigator can encounter in real observational practice.

As a contrasting example, take the study of brightness fields of a very narrow ADP, of delta-shaped type, for instance. In this case the basic relation can be rewritten as:

$$T_A = \int_{-\infty}^{\infty} P(x - x')T_B(x')\,dx' = \int_{-\infty}^{\infty} \delta(x - x')T_B(x')\,dx' = T_B(x). \tag{5.64}$$

It follows from this relation, that the instrument will precisely reproduce the brightness profile of an object. The opposite situation (frequently used in radio-astronomy) is also possible, where the bright point-like source is used as a supplementary one for determining the antenna characteristics, that is:

$$T_A(x) = \int_{-\infty}^{\infty} P(x')\delta(x - x')\,dx' = P(x). \tag{5.65}$$

Now we introduce some important spatio-spectral notions for describing the procedure of smoothing. For this purpose we shall introduce (still only formally) the Fourier transformation for functions determining the ADP and the field of a

source, in the following form:

$$\dot{S}_{\mathrm{B}}(u, v) = \int_{-\infty}^{\infty} \int_{-\infty}^{\infty} T_{\mathrm{B}}(x, y) \exp\left[2\pi \mathrm{j}(xu + yv)\right] \mathrm{d}x \, \mathrm{d}y \tag{5.66}$$

$$\dot{S}_{\mathrm{P}}(u, v) = \int_{-\infty}^{\infty} \int_{-\infty}^{\infty} P(x, y) \exp\left[2\pi \mathrm{j}(xu + yv)\right] \mathrm{d}x \, \mathrm{d}y. \tag{5.67}$$

We shall determine the obtained functions by $S_{\mathrm{B}}(u, v)$ as a two-dimensional spatial spectrum of distribution of the source brightness $T_{\mathrm{B}}(x, y)$, and $S_{\mathrm{P}}(u, v)$ as a two-dimensional spatial spectrum (or the spatial frequency characteristic) of an antenna. In this case $u$ and $v$ will be spatial frequencies in two orthogonal directions $x$ and $y$. If the whole transformation procedure occurs on the investigated surface, then the dimension of spatial frequencies will be 1/m. Quite frequently, however (for example, in radio-astronomy), the transformation procedure is performed in the so-called picture plane, while remaining in the solid space (using the polar and azimuthal angles). In this case the dimension of spatial frequencies will be $(\text{radian})^{-1}$ or $(\text{degree})^{-1}$. If the source possesses azimuthal isotropy, it is convenient to pass to the other coordinate system – the polar radius $\rho$ and the wave number $k$. In this case the appearance of the Fourier transformation will be quite different (Rytov, 1966), namely:

$$\dot{S}(k) = \int_{0}^{\infty} T_{\mathrm{B}}(\rho) \, J_0(k\rho) \rho \, \mathrm{d}\rho, \tag{5.68}$$

where $J_0(k\rho)$ is the zero-order Bessel function.

Equation (5.61) can be easily transformed into an algebraic one. Applying the two-dimensional Fourier transformation to both its parts, we obtain (see Appendix B):

$$\dot{S}_{\mathrm{A}}(u, v) = \dot{S}_{\mathrm{B}}(u, v) \, \dot{S}_{\mathrm{P}}(u, v), \tag{5.69}$$

where $S_{\mathrm{A}}(u, v)$ is the spatial spectrum of a signal recorded by an instrument. It can easily be seen that the obtained relation exactly repeats the relations we have used in analysing the propagation of electrical signals through the linear systems (and through the filters, in particular) (see section 2.6). Observational practice indicates that the source will always have a richer spectrum, and the antenna, as a filter of spatial frequencies, will remove high-frequency components (or smaller details, in other words), i.e. it will operate as a low-pass filter. The analogy with filtering systems is very important, since it opens the way to using powerful spectral methods developed in communications theory and in optics, as applied to the generalization of properties of signal transformation by antenna systems, which can now be considered as filters of spatial frequencies. The object, in its turn, can be characterized by the spectrum of spatial frequencies. As Born and Wolf (1999) have shown, a more general characteristic of the electromagnetic radiation field can also be introduced, which determines all its properties accessible to study by means of an instrument which is sensitive to quadratic-in-the-field quantities. This is a mutual coherence function, which includes both a spatial (the spatial spectrum)

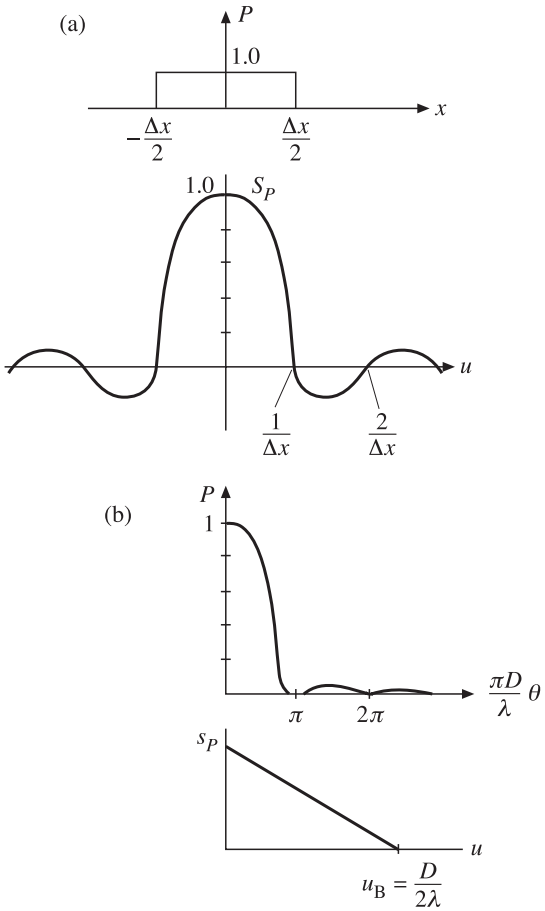


**Figure 5.10.** Examples of the relationship between antenna directional pattern (ADP) and special spectrum. (a) Ideal ADP (without side lobes zones). (b) Real ADP (with side lobes zone).

and a temporal characteristic of the radiation field of an object. The application of such a characteristic requires very serious theoretical training of the investigator; therefore, we shall refrain from the description and application of such an approach in this book.

As examples of spatial frequency characteristics of antenna systems, we shall consider two model situations. The first example is as follows. Suppose the antenna to have illuminated on an investigated surface the one-dimensional rectangular segment $\Delta x$ (Figure 5.10). Using (5.67), we shall write the expression for the spatial one-dimensional spectrum of an illuminated area:

$$S_{\mathrm{P}} = \int_{-\Delta x/2}^{+\Delta x/2} \exp\left(\mathrm{j}2\pi u x\right) \mathrm{d}x. \tag{5.70}$$

After some transformations we obtain the expression for the spatial spectrum of the area in the form of well-known function (Figure 5.10):

$$S_{\mathrm{P}} = \Delta x \frac{\sin(u\pi\,\Delta x)}{u\pi\,\Delta x}. \tag{5.71}$$

Attention should be paid to the following circumstance: the presence of infinitely high frequencies (infinitely small details) in the spatial spectrum of an illuminated area, a situation, which is, certainly, inadmissible physically. This paradox is related to the selected model for ADP – the cutoff from a cone without the presence of side lobes. As we have noted above, such a model is unrealizable physically because of diffraction effects.

Consider now the realistic (with inclusion of a side-lobe radiation) ADP model, which is often used for estimation calculations. But now we shall consider it in the angular measure:

$$P(\theta) = \left( \frac{\sin \dfrac{\pi D}{\lambda}\theta}{\dfrac{\pi D}{\lambda}\theta} \right)^2, \tag{5.72}$$

where $D$ is the diameter of a circular aperture and $\theta$ is the polar angle. From this expression we can easily obtain the total ADP value at zero points by equating the parameter to $\pm\pi$; then $\theta_0 = 2\lambda/D$. This problem can be solved also for finding the resolution from a half level, i.e. from the 3 dB level (by the graphical method, for example); then $\theta_{3\mathrm{dB}} = 1.3\lambda/D$. The performed estimations relate to the ADP model of (5.72) type only, and for other realistic forms of ADP the estimates will, of course, be a little bit different numerically.

Using (5.67), we obtain the expression for a spatial one-dimensional spectrum of realistic ADP, by making use of well-known expression for definite integrals (Gradshteyn and Ryzhik, 2000):

$$S_{\mathrm{P}}(u) = \begin{cases} \dfrac{\lambda}{D}\left(1 - \dfrac{u}{u_{\mathrm{b}}}\right), & u \le u_{\mathrm{b}}, \\ 0, & u > u_{\mathrm{b}}, \end{cases} \tag{5.73}$$

where $u_{\mathrm{b}} = D/2\lambda$.

Here it is important to note that, unlike (5.71), the expressions for a spatial spectrum of the realistic ADP is different – the real antenna does not pass high-frequency components of a signal, i.e. it operates as a low-pass filter (Figure 5.10(b)). In this case the boundary frequency is equal to the reciprocal of the total ADP value, which is just what should be expected, generally speaking. The in-depth analysis of spatial frequency characteristics of various forms of antenna aperture is presented in the book by Esepkina *et al*. (1973).

In the theory of antennas the fundamental statement proved is that any realistic antenna is always limited in spatial frequencies and, therefore, we always lose the fine information on the spatial properties of a source. This does not mean, however, that it is impossible to restore some part of the spatial information. We shall discuss this issue below. If we consider the spatial smoothing procedure in the physical

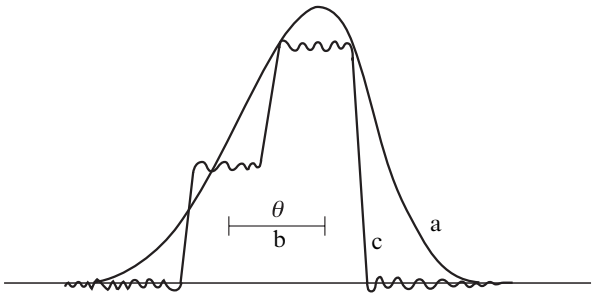


**Figure 5.11.** The restoration of a stepped signal model from the convolution of this model with the ideal ADP. (a) Result of the convolution. (b) Antenna beamwidth at 3 dB points. (c) Result of the recovery.

coordinate space, then, as we have seen, it can be described in an integral form (see equation (5.61)). This implies that it is impossible to achieve unambiguous restoration of the true (original) profile of a signal, since the regular procedure of deriving the integrand in the input signal from the expression for a prototype function for the convolution integral does not exist. If, however, we make use of the spectral-frequency presentation, then the result sought will directly follow from relation (5.69); that is to say, the spatial spectrum of the original signal will be equal to:

$$S_{\mathrm{B}}(u, v) = \frac{S_{\mathrm{A}}(u, v)}{S_{\mathrm{P}}(u, v)}. \tag{5.74}$$

And, further, using the Fourier transformation, we can reconstruct (restore) a signal in physical space:

$$T_{\mathrm{B}}(x, y) = \int_{-\infty}^{\infty} \int_{-\infty}^{\infty} \frac{S_{\mathrm{A}}(u, v)}{S_{\mathrm{P}}(u, v)} \exp\left(-\mathrm{j}2\pi(ux + yv)\right) \mathrm{d}u\, \mathrm{d}v. \tag{5.75}$$

The expression $[S_{\mathrm{P}}(u, v)]^{-1}$ is naturally called the restoring filter.

Experimental investigations and modelling have shown that such a technique 'works' most efficiently at restoring the spatial structure of a source, where its spatial features subject to study are close in their values to the spatial characteristics of an antenna. Figure 5.11 presents the result of a model example of restoring the stepped and asymmetrical model of a source from its convolution from the ADP, whose characteristic size is comparable with the angular size of the resulting response (Kostenko, 1973). Analysis of the drawing reveals a striking peculiarity, consisting in the fact that the direct analysis of a spatial form of the convolution (the response of a system) which is only slightly asymmetric does not indicate in any way that the original source is double and sharply asymmetric. The presence of sinusoidal components in a restored signal is caused by cutting off high-frequency spatial harmonics in the response spectrum while performing the Fourier-transformation procedure (5.75). This procedure has been successfully used in laboratory radiothermal test investigations both in scalar and vector representations of the relationship between the antenna radiation characteristics and the radiation properties of the

investigated media (Holmes *et al*., 1975; Truman *et al*., 1977). In virtue of the great computational expense, the framework of use of such an approach in real onboard observations is essentially limited, and the aforementioned technique has not been widely used.

The restoration procedure considered above is, however, in its essence, a far-reaching idealization of the real experimental process. This is related to the fact that in the real experiment the uncontrollable signal (noise) is always present, whose origin is caused both by the intrinsic noise of the instrument and by so-called spatial noise. The statistical properties of these components are Gaussian and do not differ from the statistical properties of an original (useful) source (certainly, in the case of radiothermal observations only). We have already discussed in detail the intrinsic (thermal) noise of an instrument and its spectral characteristics in Chapter 3. The external spatial noise (this is the conventional name) is determined by signals of those physical objects which cannot be resolved by an antenna system of the given instrument unit and, therefore, can be presented as a combination of delta-function-type sources. Such a type of signal is sometimes called the 'non-resolvable sources noise'. An excellent radio-astronomy example of such a type of signal is the radio image of the field of unresolved point-like sources presented on Plate 1. Of course, a similar situation can be found in radiothermal investigations of the Earth's surfaces (the wavy sea surface, for example, see Chapter 12). Since the measured signal and the intrinsic noise are added in power as independent signals at the receiving system's output, the intrinsic noise is sometimes transferred formally into the external spatial representation, whence the basic information is drawn, in essence (Plate 1).

Since both these components possess additivity properties with respect to the useful signal intensity, the total result can be written as:

$$T_{\mathrm{A}}(x) = \int_{-\infty}^{\infty} T_{\mathrm{B}}(x')P(x' - x)\,\mathrm{d}x' + N(x). \tag{5.76}$$

The spectral density of intensity of intrinsic and external (spatial) noise of an instrument possesses broadband properties, because these components can be presented as a set of delta-function-type sources (see section 2.5). The application of a restoring filter $[S_{\mathrm{P}}(u, v)]^{-1}$ leads in this case to the onset of (as the mathematicians say) singularities in the solution and to sharp amplification of high-frequency components (harmonics) caused by the predominating contribution of broadband noise. The situation described above is presented qualitatively in Figure 5.12. The resulting image is covered in this case by the background consisting of sharply flickering pixels of an image. Such a type of signal was called a speckle-type signal; it is well-known in television ('snow' on the TV screen in the absence of a basic signal) and in synthetizing the image in the scatterometry at reception of a backscattered signal. Certainly, the appearance of such a hindering (parasitic) signal sharply suppresses the possibilities of identification and recognition of a basic (useful) signal.

The problem considered thus relates to the class of so-called incorrectly formulated problems (Tichonov and Arsenin, 1979). A spectrum of methods is proposed for its solution. In the given case we shall indicate a fairly efficient approach, based

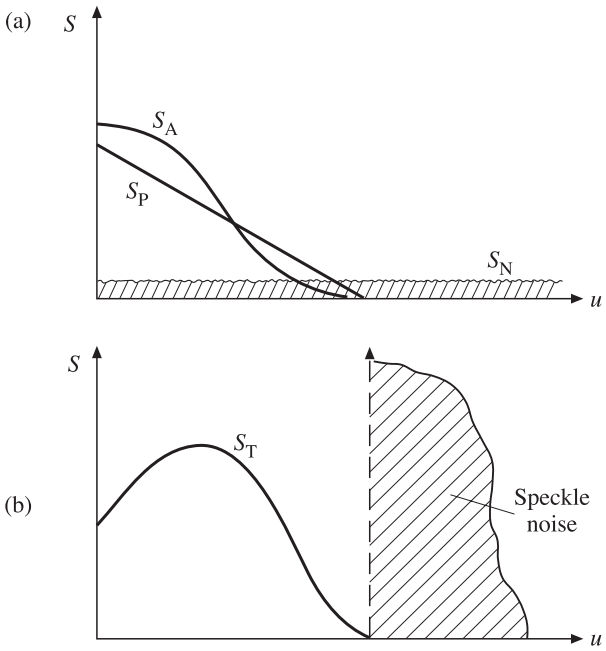


**Figure 5.12.** Qualitative picture of the restoration of a signal in the presence of noise components. (a) Spectra of antenna temperature ($S_A$), ADP ($S_P$) and noise ($S_N$). (b) The result of the recovery. See explanations in the text.

on the theory of minimizing root-mean-square prediction. In this case the best estimate (in the one-dimensional case) $\hat{T}_{B0}(x)$ of a true spatial signal $T_B(x)$ is

$$\hat{T}_{B0}(x) = \int_{-\infty}^{\infty} S_A(u)\, H_0(u) \exp(-2\pi \mathrm{j} u x)\, \mathrm{d}u, \tag{5.77}$$

where the filter $H_0(u)$ is determined by the expression

$$H_0(u) = \frac{1}{S_P(u)} \frac{|S_P(u)\, S_B(u)|}{|S_P(u)\, S_B(u)|^2 + |S_N|^2}. \tag{5.78}$$

It can be shown that such a filter ensures the minimum of a root-mean-square error of prediction:

$$\varepsilon^2 = M[\hat{T}_{B0}(x) - T_B(x)]^2. \tag{5.79}$$

Thus, $H_0(u)$ describes the optimum characteristic of a restoring filter of spatial frequencies. It can be seen from expression (5.78), that the numerator and denominator of this relation include the power spectrum of a true signal, distorted by the linear instrument in the absence of noise, and the power spectrum of the noise itself. For each spatial harmonic of the signal spectrum obtained from the experiment, there exists a superposition of the corresponding noise power and the original signal

filtered by the instrumental function. Therefore, the filter (5.78) can be constructed, provided that it is possible to separate the aforementioned spectral components of the resulting signal observed. Therefore, the principal problem for the processing software lies in finding the estimates (of polynomial type usually) for $|S_N(u)|$ and $|S_P(u)\, S_B(u)|$ by approximating them in the spectral region by the least squares method using the *a priori* information on the original source structure. The success in restoring the radio-astronomical signals by the aforementioned method (and by ideologically close procedures) are quite impressive for today. There is no doubt, that this type of procedure will be widely applied in the very near future in the field of microwave remote sensing as well.

## 5.8 OUTDOOR CALIBRATION OF RADIOMETER INSTRUMENTS: THE METHOD OF CONTRASTING HALF-SPACES

As we have already noted, the procedure of reception and recording of radiothermal emission has some peculiarity (with respect to radio communications, television, radar), related to the physical features of the radiothermal emission of studied objects and of the receiving system itself.

For these reasons calibration procedures occupy a specific place in microwave sensing. They are subdivided, in essence, into two parts; the calibration of the receiving device itself (the determination of absolute scales, the sensitivity; see Chapter 3) (the indoor calibration, conventionally) and the calibration of the antenna system and antenna transmission line (the outdoor calibration). The indoor calibration is usually performed by means of two calibration (internal) sources, which are situated constructively just inside the receiving onboard satellite instruments and operate according to some particular, prespecified programme. The outdoor calibration is a considerably more complicated procedure, since the design philosophy of a flight vehicle (aircraft or satellite) and the features of antenna system mounting on a flight vehicle can essentially change the antenna field characteristics in the side-lobe zone. Thoroughly performed indoor and outdoor calibrations make possible the so-called absolute measurements, i.e. the antenna temperature transferring to the radiobrightness temperature of an investigated object (certainly, with regard to its geometrical properties). In some cases, however, there is no necessity to obtain the absolute values of a signal. In some measurements it is important to obtain the contrast in the values of a signal, taking into account that all remaining parameters of a system and ambient space remain virtually unchanged. Such a type of measurement was called relative measurement. In the process of real full-scale investigations, both the first and second type of measurement is used, depending on the particular situation. In some cases the combined approach to the solution of experimental problems is required.*

* Note here that there is no generally accepted treatment of notions of absolute and relative measurements, and some authors give different physical meanings to these notions.

Even at the first stage of radiothermal investigation of terrestrial surfaces (1967–1973) (see Chapter 14), when the normalized sensitivity of onboard radiometers was 1.5–2 K, the necessity for detailed analysis of the radiation field of an antenna system, with regard to the features of antenna mounting on a flight vehicle, was fully recognized (Rabinovich *et al.*, 1968, 1970). In the mid-1970s, the appearance of onboard highly sensitive radiothermal satellite instruments (with normalized sensitivity of up to 0.03–0.1 K) (Amirkhanyn *et al.*, 1975) put on the agenda the necessity of developing an efficient technique of absolute and relative radiothermal measurements in the regime of direct onboard observations. On the basis of many years of experience of processing the experimental data of onboard observations, the author of this book proposed in 1975, and then verified in the course of a series of onboard experimental works, the special technique of processing the radiobrightness registrograms with the purpose of obtaining estimates of important antenna parameters (the scattering coefficient, the background radiation in the side-lobe zone, the main lobe width) in the regime of direct onboard measurements (Veselov *et al.*, 1981). The proposed technique is based on the transparent physical idea that, when the flight vehicle passes through two sharply contrasted (in the radiobrightness sense) semi-infinite surfaces (from sea to land, for instance), the radiothermal signal registrogram gives a peculiar picture of the transition signal, which can reveal the integral features in the radiation field of an antenna system. This method, called the method of contrast half-spaces (MCH), has been actively used since in various modifications, for example, for restoring the main lobe of ADP of onboard satellite instruments (Savorskii *et al.*, 2000). Another interesting example of using this method is the calibration of active–passive satellite instruments of the interplanetary Cassini spacecraft (in the International Cassini mission) at a gravity-assist during its Earth swing-by on its further journey to Saturn. The ground track of the instrument's ADP passed over the surface of Pacific Ocean and over the abrupt transition at the ocean–land boundary (with South America). The radiometric and scatterometric parts of satellite instruments were calibrated from the radiothermal and backscattered ocean–land contrast (West *et al.*, 2000).

A fairly complicated signal (see relations (5.37) and (5.50)) arrives at the radiometric receiver's input, the useful information being contained, in essence, in a single component ($T_{AB}$) only. Its value is determined by the signal energy reception at the main lobe of an antenna, since the position of the latter in space is quite well known. But the information, which comes into the side-lobe zone ($T_{SB}$) is, actually, difficult to use, since the characteristics of antenna radiation in these DP zones are virtually unknown to a sufficient accuracy (because the side-lobe radiation is sensitive to design features of a particular specimen of antenna and to the features of its mounting on a carrier). Besides, it is difficult to unambiguously interpret the signals coming to the side-lobe zone from their spatial position relative to the antenna carrier. An indicative illustration of this statement is the registrogram of a radiothermal signal recorded in passing through the land–water transition (and back) over Lake Ladoga by means of high-sensitivity radiometric R-2 satellite instruments (at the working wavelength of 2 cm) installed on the Russian IL-18 aircraft-laboratory (Figure 5.13). The signal structure in the $2'$ zone of the 'water–

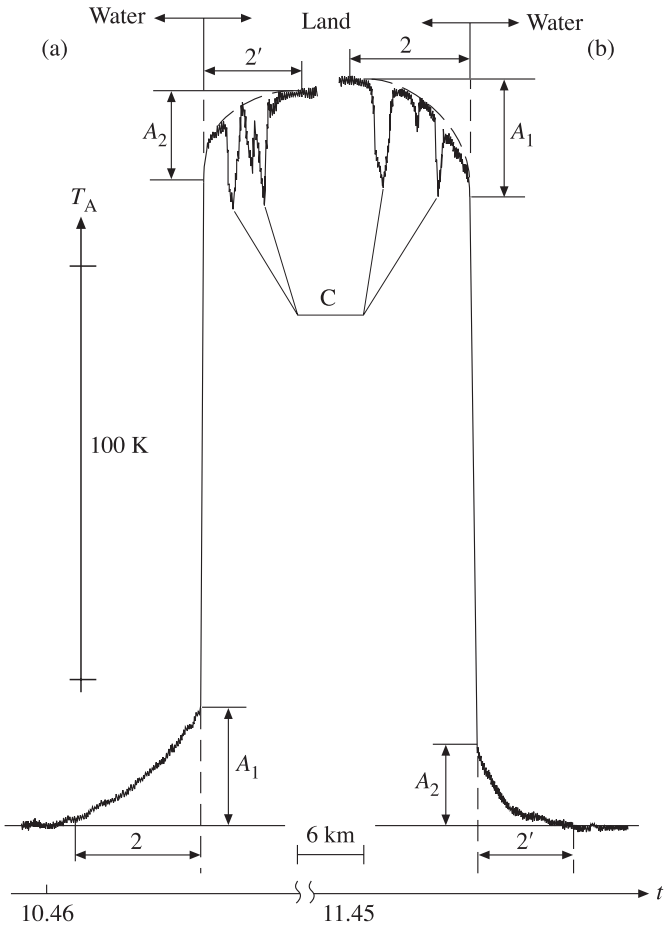


**Figure 5.13.** Fragments of the output radiometer signal of airborne (Russian IL-18) instruments (radiometer R-2) when crossing a water–land transition. The working area is Lake Ladoga (Russia). The working date was 9 September 1975. The flight height is 4000 m. Moscow time and spatial scale are shown on abscissa. Temperature scale is shown on ordinate. See notation $A_1$, $A_2$, C, 2, $2'$ in the text. (a) Water–land transition. (b) Land–water transition.

land' fragment (Figure 5.13(a)) and in the 2 zone of the 'land–water' fragment (Figure 5.13(b)) is determined by simultaneous reception (by an antenna) of radio-emission from highly separated (in the physical space) fragments of radiothermal background of the surface: a smoothly varying signal component (shown by the dashed line on the drawing) is caused by reception of emission from the land in the side-lobe zone, whereas the strong negative variations (defined by C) are caused by reception of emission from the land elements at the main lobe. The contribution to the total signal from emission reception at the side lobes in the forward half-space from the land–water contrast is designated by symbol $A_1$, and the same contrast at

the side lobes in the backward half-space by symbol $A_2$. At the return passage (Figure 5.13(b)) through the same geographical region the situation was, certainly, mirrored. It can easily be seen that the given antenna system of the satellite instruments possesses small integral asymmetry of forward and backward half-spaces of emission in the side-lobe zone.

Thus, the total (over the whole observational half-space $2\pi$) Fourier restoration (as it can be performed for laboratory investigations) is not possible at all in the onboard version. The information parameter subject to measurement is the quantity $T_{AB}$ and its variations, which should be discriminated against the background of variations of $T_{SB}$ and noise signals of an antenna and transmission line (with losses), which are statistically indiscernible from the basic signal. For this reason there is no necessity, from the practical point of view, to perform the total (and very laborious) Fourier restoration of antenna parameters.

Thus, the absolute measurements of $T_{AB}$ can be performed through knowledge of the indoor calibration of a radiometer (for example, the scale and radiobrightness temperature of an equivalent), the performance coefficient and temperature of the antenna transmission line (ATL), and the antenna scattering coefficient and radiobrightness temperature of the underlying surface, whose emission is accepted at side lobes, i.e. the $T_{SB}$ value.

The difficulties, associated with accounting for the transmission line's performance coefficient and temperature profile, can either be taken into account in experimental practice, or eliminated by appropriate design solutions. The most radical way of doing this is by the total thermal stabilization of the ATL, the antenna and the high-frequency part of a radiometer, by the use of antennas with maximum performance coefficient and by the design matching of the radiometer's input unit with the antenna. Here the latter term is constant and can be taken into account at processing or at preliminary calibration. It can also be seen from these considerations, that, in performing absolute measurements, even under these most favourable conditions, the difficulty arises in determining the scattering coefficient – under onboard conditions – and the quantity $T_{SB}$, which is determined by the type of surface and ADP in the side-lobe zone.

In performing, however, the relative (within the limits of the given working mission and with the same type of homogeneous surface) measurements and under the condition of small variations of radiobrightness, knowledge of the ATL scattering coefficient and performance coefficient is required. In other words, the signal variation at the main lobe $\Delta T_{AB}$ is related to the measured variation of $\Delta T_A$ as follows:

$$\Delta T_{AB} = \frac{\Delta T_A}{(1-\beta)\eta}. \tag{5.80}$$

Thus, for performing the correct absolute and relative onboard radiothermal experiments it is necessary to measure and verify, to an accuracy sufficient for practical purposes, the following parameters:

(a) the ADP main lobe value;
(b) the scattering coefficient value;

(c) the value of $T_{SB}$ of various surfaces for the given antenna specimen and its design features.

As we have noted above, the scattering coefficient is the antenna system characteristic, whose value depends both on a particular specimen of antenna, and on a series of design features of the antenna mounting on the flight vehicle (the method of fastening, the shape of the fairing, etc.). The ground or laboratory verification of such a parameter is fairly labour-consuming for natural reasons, though in some critical cases it is carried out on flight vehicle models (Rabinovich *et al.*, 1970). For this reason it is desirable to find the method of determination (or estimation to an acceptable accuracy) of the scattering coefficient under onboard conditions and its regular re-verification in the course of lengthy flight experiments. The data on the beam efficiency (i.e. the quantity $1 - \beta$) of radiometric space satellite instruments presented in the literature (see, for example, Njoku *et al.*, 1999; Mo, 1999), are the result of calculations from ground measurement data, but in no way the result of real observations. With the modern technology of antenna systems production, the extreme values of scattering coefficients for immovable antennas equal 3–10% (unique samples) and 10–15% (standard samples). For scanning systems with an immovable irradiator the scattering coefficients increase up to 10–15% (unique samples) and 15–20% (standard samples). In general, it should be mentioned, the methods of minimizing the scattering coefficient for various types of antennas are but weakly developed so far. The available data in the specialized radio-engineering literature give only rough classification of antennas in average values of a scattering coefficient. Detailed analysis has shown that it is horn and horn-parabolic antennas which best satisfy all the requirements formulated above. These antennas possess minimum scattering coefficient value and maximum performance coefficient (PC), up to 98–99%; they can also be well coordinated in the necessary band and constructively integrated with the microwave receiver set into a single thermally stabilized unit (Amirkhanyn *et al.*, 1975; Strukov and Skulachev, 1984, 1986; Cherny and Chernyavsky, 2001; Njoku *et al.*, 1999; Mo, 1999; Ruf, 2000a,b). It is interesting to note that the cophased array version, which was used for the microwave unit of Nimbus 5 and 6 satellites (Allison *et al.*, 1974), has now been completely rejected for potential satellite instruments because of the small performance coefficient of such antennas, the single-frequency mode of operation and the rather high value of the scattering coefficient. Preference is now for the horn and parabolic types of antennas with the mechanical mode of scanning with conical geometry (see Chapter 14).

As far as the brightness values of various surfaces are concerned, the situation is rather complicated. As the special ground experiments have shown, the averaged value of radiobrightness temperature, falling on side lobes, is approximately 10–30% lower than the value received by the main lobe. However, the question of measuring this quantity and its statistical characteristics still remains open in the case of onboard experiments, where the surface (with unknown radiobrightness characteristics, in the general case) is investigated by means of an antenna for which the ADP in the side-lobe zone is also known with high uncertainty. True, experimental practice is more hopeful. This is due to the fact that the reception in the side-lobe

zone is accomplished in a fairly wide solid angle (of the order of $2\pi$), and for this reason the averaged value of temperature fluctuates quite insignificantly for the given type of surface. This allows us to use the averaged $T_{SB}$ value for absolute measurements, and for relative measurements, within the limits of a straight flight over sufficiently homogeneous surfaces, $T_{SB}$ can be considered to be constant. Thus, it seems apparently impossible to escape the limits of $\pm 10$ K in the absolute onboard measurements without using the *a priori* information on radio-emission of the surface and special techniques for determining the emission received in the side-lobe zone, and also without checking the scattering coefficient value. In performing ground-based laboratory radiothermal experiments the technique of calibration of a measurement system by the 'black-body', 'artificial zenith' and a quiet water surface allows us to reasonably reliably determine the scattering coefficient of an antenna and the side-lobe emission $T_{SB}$ (certainly, within the given conditions of performing the experiment). The accurate implementation of a similar technique allows us to achieve an accuracy of up to 0.2 K (or 0.3%) at laboratory absolute measurements of water surface emission,* as compared to the theoretical radiobrightness value calculated on the basis of modern data on dielectric characteristics of water (see Chapter 8).

The special technique of graphical processing the registrograms received from the surfaces, which highly differ in the radiothermal sense, is considered below. This processing allows us to evaluate the aforementioned parameters to an acceptable accuracy ($\approx$5–10%) and to verify them in a regular manner under onboard conditions without disassembling the antenna systems.

Figures 5.14 and 5.15 present fragments of registrograms of the channel of the R-18 radiometer installed on the Russian IL-18 aircraft-laboratory (see Chapter 14), at the working wavelength of 18 cm, at transition through two highly contrasted radiothermal zones of the earth's surface: the fresh water Balkhash and Ladoga lakes and the land. The antenna represents a cutting-off from a parabolic cylinder with a vibrator power supply and with the main lobe width (on the 3 dB level) of 18°. The experiment was performed in such a manner, that the intersection of the water–land interface boundary took place in the same geographical region, but at various heights of the carrier (aircraft) – from 600 m to 4300 m. Here Figure 5.14 presents the fragments of a registrogram of a land–water transition (in one direction) (Lake Ladoga) and Figure 5.15 the fragments of a registrogram of a water–land transition and and a return run over the same geographic region, a land–water transition (Lake Balkhash). The qualitative analysis of registrograms (Figures 5.13–5.16), obtained in different geographical zones and by various remote sensing instruments, shows, nevertheless, that the character of radiothermal signals at sharp transitions is quite similar. The presence of two zones are represented: a zone of slow signal variation and a zone of rapid signal variation. Depending on the experiment geometry, the clearness of these zones on the registrograms is certainly different: the higher the vehicle flight altitude, the clearer the zones. This feature is especially well seen

* Experiments were performed in 1976 under the direct guidance of the author of this book (Bordonskii *et al.*, 1978).

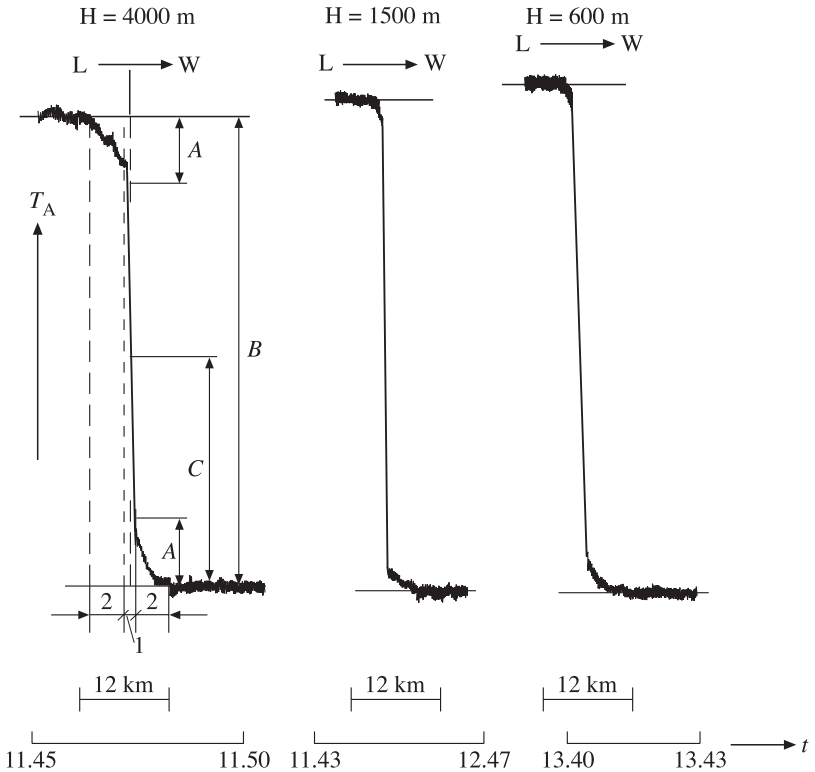


**Figure 5.14.** Fragments of the output signal of airborne (Russian aircraft-laboratory IL-18) radiometer R-18 ($\lambda = 18$ cm) when crossing a land–water transition at various heights ($H = 4000$ m, 1500 m and 600 m). The working area is Lake Ladoga (Russia). The working date was 9 September 1975. Moscow time and spatial scale are shown on abscissa. See notation A, B, C, 1, 2 in the text.

on the registrograms in Figure 5.16, where the results of flights at the land–water transition (in one direction) at different altitudes (Lake Ladoga, instrument R-2) are presented. To clear up the situation, we shall consider the simplified geometry of the experiment whose flight part is shown schematically in Figure 5.17(a), where $\Omega'$ and $\Omega''$ are solid angles of the main and side lobes directed to the land. Figures 5.17(b) and (c) presents schematically the registrograms of the radiothermal signal of the land–water transition with separation of some characteristic zones. The analysis of radiothermal registrograms of highly sensitive radiometers, obtained in flight through the transition between two highly contrasting (in the radiothermal sense) surfaces (such as a quiet water surface and a homogeneous rocky coast), shows the presence of two prominent zones (in the corresponding time scale of recording): the prolonged zones with a smooth signal variation (zones 2 and $2'$) (Figures 5.17(b) and (c)) and the zone of rapid and virtually linear drop (zone 1). Zones 2 are formed when the radio-emission of a contrasting half-space is generated within the solid

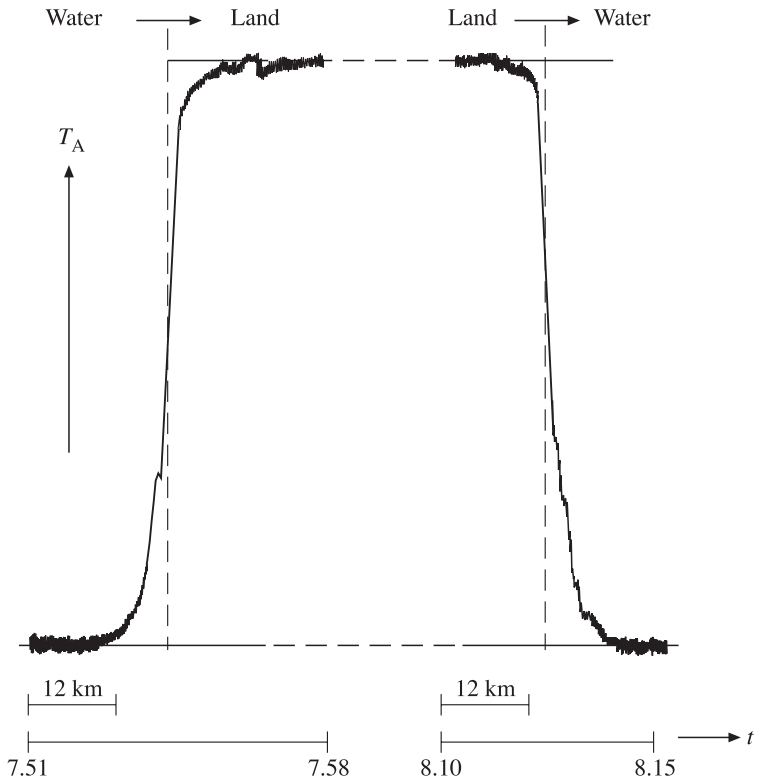


**Figure 5.15.** Fragments of the output signal of airborne radiometer R-18 when crossing a water–land and a land–water transition. The working area is Balkhash Lake. The flight height is 4300 m. The working date was 25 April 1975. Moscow time and spatial scale are shown on abscissa.

angle of the side antenna emission, and zone 1 when the same radio-emission is generated within the solid angle of the main lobe. Figure 5.17(c) presents schematically the case where the main lobe width is extremely small (the delta-function), and the side emission remains at the same level (as is observed in the real experiment; see Figure 5.16). As the experiments have shown, zones 2 are virtually symmetrical for many types of antenna used; and this indicates that the side-lobe radiation of antennas, averaged in solid angles into the forward and backward half-spaces, are generally equal.

With regard to expressions (5.37)–(5.40) and (5.50), obtained above, the antenna temperature of an onboard instrument at the time the flight vehicle intersects the water–land boundary by a flight vehicle can be written as:

$$T_A = [T_{ABL}\beta' + T_{ABW}(1-\beta')](1-\beta)\eta + T_{SBL}\beta''\eta + T_{SBW}(\beta-\beta'')\eta + T_0(1-\eta), \tag{5.81}$$

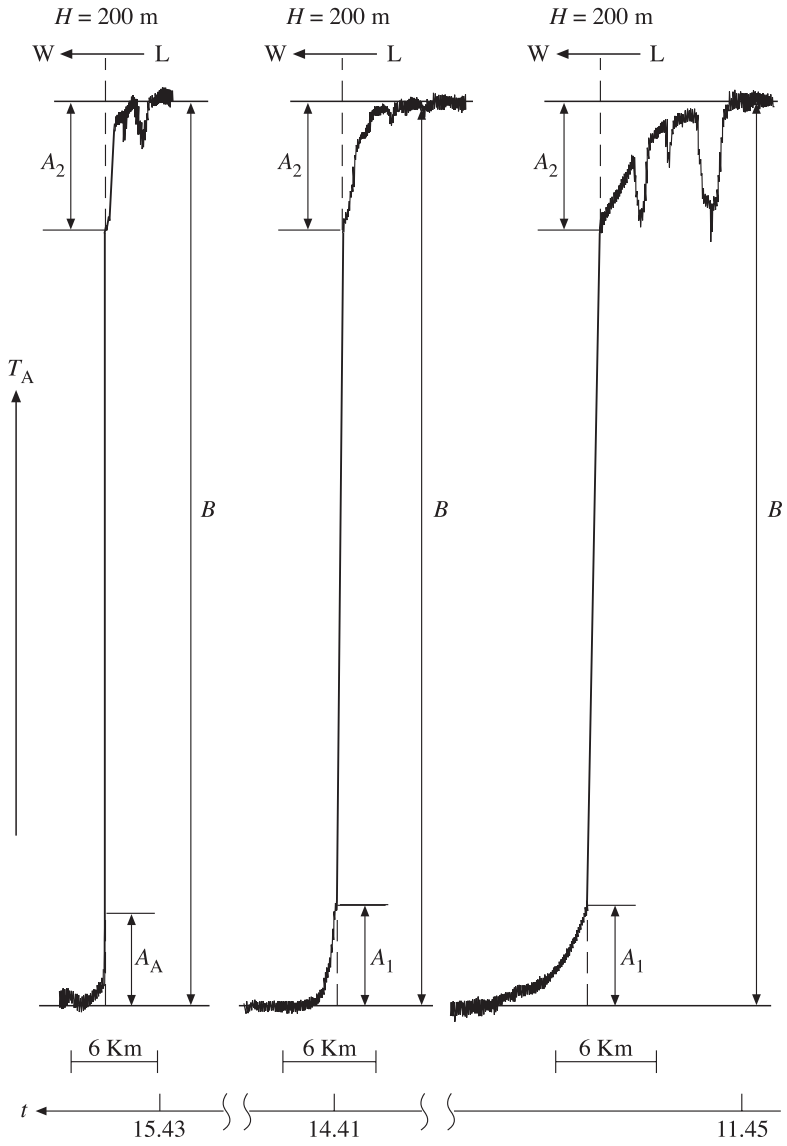


**Figure 5.16.** Fragment of the output signal of airborne radiometer R-2 when crossing a land–water (L–W) transition at various heights ($H = 4000$ m, 600 m, 200 m). See notation $A_1$, $A_2$, B in the text. Legends as for Figure 5.13.

where $T_{ABL}$, $T_{ABW}$ are the radiobrightness temperatures received at the main lobe from the surface of land and water, respectively; $T_{SBL}$ and $T_{SBW}$ are the radiobrightness temperatures received in the side-lobe zone from the surface of land and water, respectively. Quantities $\beta'$ and $\beta''$ are the scattering coefficients of a

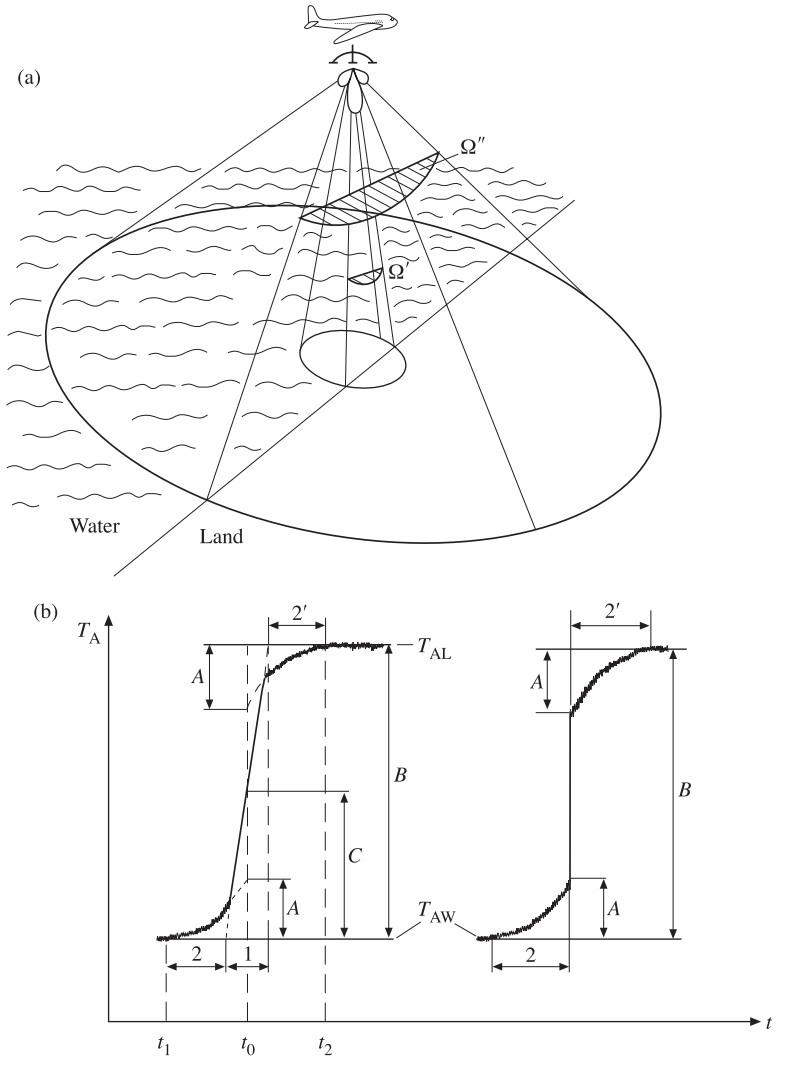


**Figure 5.17.** Schematic presentation of a water–land transition airborne experiment. (a) Simplified geometry of the experiment. (b) Qualitative picture of output radiometer signal (in arbitrary units). (c) Output signal when a main lobe zone is a delta-function. See notation in the text.

part of the main lobe and of the side-lobe zone, directed to the land surface, and they can be expressed as

$$\beta' = \frac{\iint_{\Omega'} P\,\mathrm{d}\Omega}{\iint_{\Omega_{AB}} P\,\mathrm{d}\Omega}; \beta'' = \frac{\iint_{\Omega''} P\,\mathrm{d}\Omega}{\iint_{4\pi-\Omega_{AB}} P\,\mathrm{d}\Omega}. \tag{5.82}$$

From the analysis of relation (5.81) it can easily be seen that, irrespective of absolute values of brightness temperatures of contrast half-spaces, the character of antenna temperature $T_A$ of the transition will be symmetrical (if the side emission of an antenna is symmetrical integrally), in the linear part of a registrogram (zone 1) the main contribution being made by the first term (5.81), and in zones 2 by the second one. The expression for the antenna temperature value for a middle of transition $T_{AM}$ (at time instant $t_0$ in Figure 5.17(b)) is equal to:

$$T_{AM} = \frac{T_{ABL} - T_{ABW}}{2}(1 - \beta)\eta + \frac{T_{SBL} - T_{SBW}}{2}\beta\eta + T_0(1 - \eta). \tag{5.83}$$

In the case where the whole solid angle of an antenna is directed to one of contrast half-spaces (far from the transition), the expression for antenna temperature can be presented as ($T_{AL}$ at a flight over the land and $T_{AW}$ over the water):

$$\begin{aligned} T_{AL} &= T_{ABL}(1 - \beta)\eta + T_{SBL}\beta\eta + T_0(1 - \eta) \\ T_{AW} &= T_{ABW}(1 - \beta)\eta + T_{SBW}\beta\eta + T_0(1 - \eta). \end{aligned} \tag{5.84}$$

Now we shall consider the features of transition registrograms. These features include (see Figures 5.13–5.14, 5.16 and 5.17) the value of the total antenna temperature drop between two contrasting surfaces $B$ and the contribution $A$ of a contrast between the surfaces to the forward and backward half-spaces of a side-lobe zone (these zones are shown schematically in Figure 5.17(a)). The total brightness contrast of the land–water transition, recorded at instrument's output, will be:

$$B = T_{AL} - T_{AW} = (T_{ABL} - T_{ABW})(1 - \beta)\eta + (T_{SBL} - T_{SBW})\beta\eta. \tag{5.85}$$

The brightness contrast contribution from surfaces into the side-lobe zone (into the forward and backward half-spaces separately) will be equal to:

$$A = (T_{SBL} - T_{SBW}))\frac{\beta}{2}\eta. \tag{5.86}$$

The parameters directly measured at the instrument's output are the values of antenna temperatures $T_A$ (relations (5.81) and (5.84)), which can be determined by using the indoor calibration of a radiometer. In their turn, $T_0$ and $\eta$ can be obtained from the data of measurement of the antenna transmission line temperature and from the preliminary (pre-flight) measurements, for example, by the method of two loads (see Chapter 7). The principal unknown quantities remain the values of the antenna scattering coefficient (under specific conditions of its installation on the given flight vehicle) and the averaged values of brightness temperatures of contrast surfaces in the side-lobe zone for the given antenna (5.39). However, as detailed studies of this problem have shown (Veselov *et al.*, 1981), the situation is not desperate. The fact is, that the contrasts between brightness temperatures, measured at the main lobe and at the side-lobe zone, are very close:

$$T_{SBL} - T_{SBW} \approx T_{ABL} - T_{ABW}. \tag{5.87}$$

This equality is observed to an accuracy better than 5%. In this case $\beta$ and its components into the forward $\beta_F$ and backward $\beta_B$ half-spaces can be estimated, in the first approximation, directly from the transition registrogram geometry (Figures 5.16 and 5.17):

$$\beta = \frac{2A}{B}; \beta_F = \frac{A_1}{B}; \beta_B = \frac{A_2}{B}. \tag{5.88}$$

It is important to note that the given estimate does not depend either on the internal scale of an output instrument or on the value of losses in the antenna line.

### 5.8.1 MCH procedure

To construct the correct procedure for the method of contrasting half-spaces (MCH) and for further calculations of the receiving system's parameters it is necessary to specify, proceeding from theoretical estimates (see Chapter 8), the value of $T_{ABW}$ and use the proposed iteration procedure ('a ring') to clear up the physical substantiation of the theoretic value. So, the following procedure is proposed:

(1) First we perform the preliminary estimation of $\beta$ from the transition registrogram (expression (5.88)).
(2) Then, specifying the theoretical value of $T_{ABW}$ and the estimate of $\beta$, we obtain the $T_{SBW}$ value by the following formula:

$$T_{SBW} = \frac{1}{\beta\eta}[T_{AW} - T_0(1-\eta) - T_{ABW}(1-\beta)\eta]. \tag{5.89}$$

(3) Using the obtained $T_{SBW}$ value, we find $T_{SBL}$ according to the expression:

$$T_{SBL} = \frac{2A}{\eta\beta} + T_{SBW}, \tag{5.90}$$

where the value of $A$ is taken on the indoor calibration scale.
(4) Using the obtained value of the total drop (in the indoor scale) and the theoretical value of $T_{ABW}$, we obtain the estimate for $T_{ABL}$:

$$T_{ABL} = \frac{B-2A}{\eta(1-\beta)} + T_{ABW}. \tag{5.91}$$

(5) Using the results of steps (1) and (2), we obtain the second (improved) estimate for the $\beta'$ value:

$$\beta' = \frac{2A}{T_{SBL} - T_{SBW}} \frac{1}{\eta}. \tag{5.92}$$

(6) Proceeding from the measured value of $T_{AW}$ and obtained values of $T_{SBW}$ and $\beta'$, we calculate the $T'_{ABW}$ value by formula:

$$T'_{ABW} = \frac{1}{\eta(1-\beta)}[T_{AW} - T_0(1-\eta) - T_{SBW}\eta\beta] \tag{5.93}$$

for further comparison with the theoretical value.

**Table 5.2.** Antenna characteristics of microwave instruments onboard airplane-laboratory IL-18 (1975–1976)

| Radiometer design | Working wavelength, cm | Sensitivity, $\tau = 1$ sec | Antenna type; aperture dimension, cm | $\theta_{3dB}$ degree of circle (calculated) |
|---|---|---|---|---|
| R0.8 | 0.8 | 0.08 | Parabolic antenna; 30 | 1.9 |
| R2 | 2 | 0.04 | Parabolic antenna, with displaced irradiator; 100 | 1.4 |
| R8 | 8 | 0.05 | Horn-parabolic antenna; 65 | 9.0 |
| R18 | 18 | 0.4 | Cage-parabolic antenna with dipole irradiators; $70 \times 70$ | 18 |

(7) Using the obtained value of $\beta'$, we obtain the restoring coefficient for relative measurements (see expression (5.81)):

$$k_R = \frac{1}{(1-\beta')\eta}. \tag{5.94}$$

As an example, we shall perform the indicated procedure for the experimental data of the R18 (I, II) instrument (see Chapter 14 and Table 5.2).

(I). The flight took place on 25 April 1975, over Lake Balkhash and the steppe regions adjacent to it. The brightness temperatures of the water surface and land (on the indoor scale) were 164 K and 267 K, the performance coefficient of an antenna transmission line was estimated (from the ground measurements) as 0.66, $T_0 = 280$ K (the in-flight measurements) (Figure 5.15).

The execution of the indicated procedure gives the following results:

(1) The estimation of a scattering coefficient gives the value of 0.27.
(2) $T_{SBW} = 95$ K (with the theoretical value of $T_{ABW} = 108$ K).
(3) $T_{SBL} = 251$ K.
(4) $T_{ABL} = 264$ K.
(5) $\beta' = 0.264$.
(6) $T'_{ABW} = 107.5$ K.
(7) $k_R = 2.04$.

(II). The flight took place on 9 September 1976, over Lake Ladoga and rocky regions adjacent to it. The brightness temperatures of the water surface and land (on the indoor scale) were 182 K and 272 K, the performance coefficient of the antenna transmission line was estimated (from the ground measurements) as 0.57 (the design

modifications in the antenna system installation took place in April 1975), $T_0 = 275\,\mathrm{K}$ (the in-flight measurements) (Figure 5.14).

The execution of the indicated procedure gives the following results:

(1) The estimation of a scattering coefficient gives the value of 0.31.
(2) $T_{\mathrm{SBW}} = 116\,\mathrm{K}$ (with the theoretical value of $T_{\mathrm{ABW}} = 110\,\mathrm{K}$).
(3) $T_{\mathrm{SBL}} = 274\,\mathrm{K}$.
(4) $T_{\mathrm{ABL}} = 267\,\mathrm{K}$.
(5) $\beta' = 0.308$.
(6) $T'_{\mathrm{ABW}} = 111.9\,\mathrm{K}$.
(7) $k_{\mathrm{R}} = 2.54$.

The comparison of theoretical values of the brightness temperature of the water surface with the measured value proves the reliability of the procedure. In addition, it follows from the obtained data that the basic approximation (5.87) is satisfied to an accuracy better than 2%.

Attention should be paid to the fact that all iterative steps must be executed and mutually verified. And, in addition, analysis of the physical sense of results is necessary, since in some cases the peculiarity of the initial data can lead to 'falling' on a diverging branch of the iteration ring, which can give physically meaningless results (such as $\beta > 1$). The indicated procedures can easily be executed onboard the flight vehicle by means of special processing units.

### 5.8.2 Estimation of the main lobe width

From the graphical representation of a radiothermal signal we can obtain one more important characteristic: the estimation of the angular size of the main lobe under onboard conditions. It can easily be seen that zone 1 (Figure 5.17(b)) in the angular measure characterizes the total main lobe width, and from simple geometrical considerations it is possible to obtain a satisfactory estimate of the main lobe width (by the 0 dB level, i.e. the full lobe):

$$\theta_{0\mathrm{dB}} = 2\mathrm{arctg}\frac{V\,\Delta t}{2H}, \tag{5.95}$$

where $\Delta t$ is the time of passage through zone 1 (Figure 5.17(b)) and $V$ and $H$ are the velocity and altitude of the carrier. And, since for the majority of beam antennas the $2.3\theta_{3\mathrm{dB}} = \theta_{0\mathrm{dB}}$ relation is valid to an acceptable accuracy, we obtain the following estimate for the main lobe value by the 3 dB level:

$$\theta_{3\mathrm{dB}} = \frac{V\,\Delta t}{2.3H}. \tag{5.96}$$

The comparison of the estimates, found by the indicated method and calculated proceeding from the design data (Table 5.2 and 5.3), shows satisfactory correspondence. In conclusion, we consider briefly the typical errors. For example, Vinogradov (1976) completely arbitrarily takes for the spatial resolution on the surface a quantity equal to half of the total transition, i.e. $\frac{1}{2}\{(t_2 - t_1)V\}$ (see Figure 5.17(b)), which

**Table 5.3.** Measured antenna characteristics of microwave instruments by the MCH method

| Time and location of experiments | Radiometer design | $\theta_{3dB}$ (calculated) degree of circle | $\theta_{3dB}$ (measured) and RMS, degree of circle | Scattering coefficient, (measured) and RMS |
|---|---|---|---|---|
| 25 April 1975; Lake Balkhah | R18 | 18 | $18 \pm 0.5$ | $0.20 \pm 0.03$ |
| 9 September 1976; Lake Ladoga | R18 | 18 | $18 \pm 0.5$ | $0.24 \pm 0.03$ |
| | R2 | 1.4 | | $0.26 \pm 0.03$ |
| 13 July 1976; the Barents Sea | R8 | 9 | $9.3 \pm 0.3$ | $0.25 \pm 0.05$ |
| | R2 | 1.4 | $2.2 \pm 0.2$ | $0.27 \pm 0.05$ |
| | R0.8 | 1.9 | $2.5 \pm 0.2$ | $0.21 \pm 0.05$ |

more than twice exceeds the design value of a spatial resolution (the half of zone 1). However, the estimation we have carried out by the proposed technique for the 'Nimbus-5' spacecraft from the land–water transition registrograms, contained in the paper mentioned, gives the value of 25–27 km. This estimate fully agrees with the design spatial resolution values found proceeding from the spacecraft antenna parameters measured on the Earth. Thus, Vinogradov's (1976) concept of finding the spatial resolution as a half of the transtion length should be recognized to be wrong and his strong criticism of 'Nimbus-5' spacecraft developers to be unsubstantiated. Similar errors, nevertheless, have been repeated in some publications, including Western literature.

### 5.8.3 Geometry of position of beams of multifrequency instruments

The accurate timing of centres of transition registrograms for multifrequency instruments allows us to solve one more important problem – of the mutual spatial-angular position of centres of antenna directional patterns for various transition lines (channels). For an example of the solution of such a problem we take the result of the following experiment on studying the mutual position of ADP centres of multifrequency radiothermal airborne instruments of the IL-18 aircraft-laboratory (Table 5.2) (Amirkhanyn *et al.*, 1975; Bespalova *et al.*, 1976a,b, 1979; Antonov *et al.*, 1995). The ADP axes for the channels of 0.8, 2, 8 and 18 cm are presented in Figures 5.18 and 5.19. Note that it is impossible to reveal these geometrical features by any other experimental method.

## 5.9 ANTENNA PARAMETERS OF AIRBORNE MICROWAVE INSTRUMENTS

As an example of using the proposed technique, we shall consider the estimation (by means of the MCH method) of antenna parameters of airborne, high-sensitivity

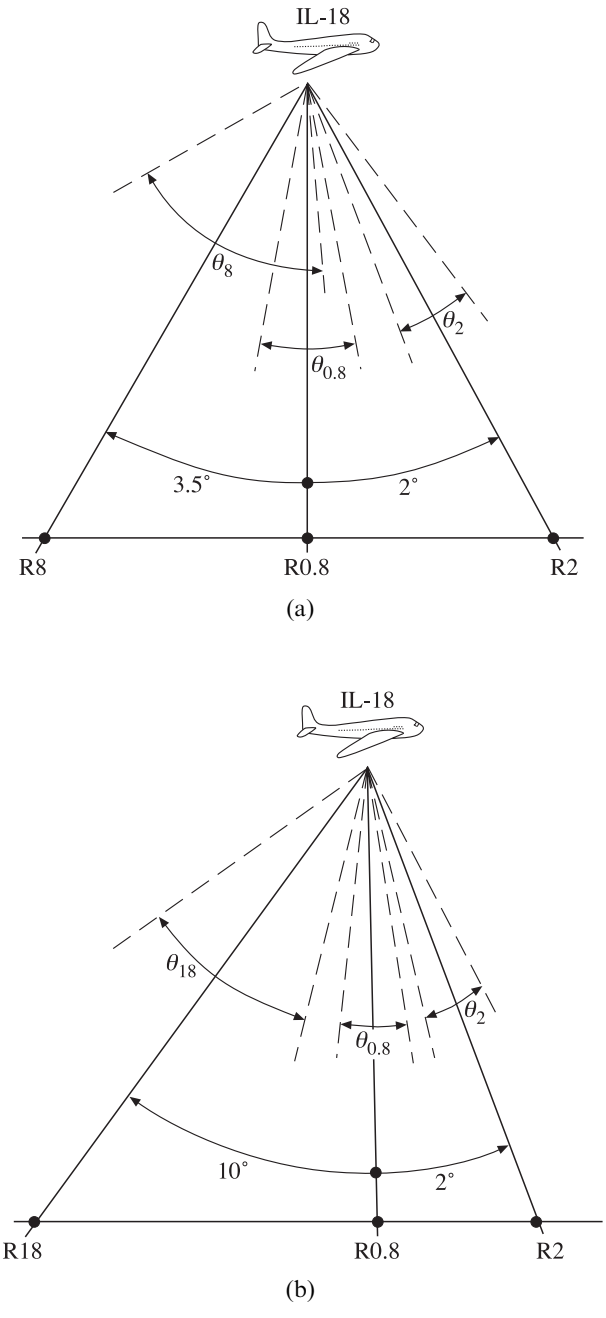


**Figure 5.18.** Schematic presentation (in no scale) of geometry for main axes and values of ADP main lobes of radiometric instruments onboard Russian aircraft-laboratory IL-18 (September 1975–July 1976): (a) for radiometers R2; R0.8; R8; (b) for radiometers R2; R0.8; R18.

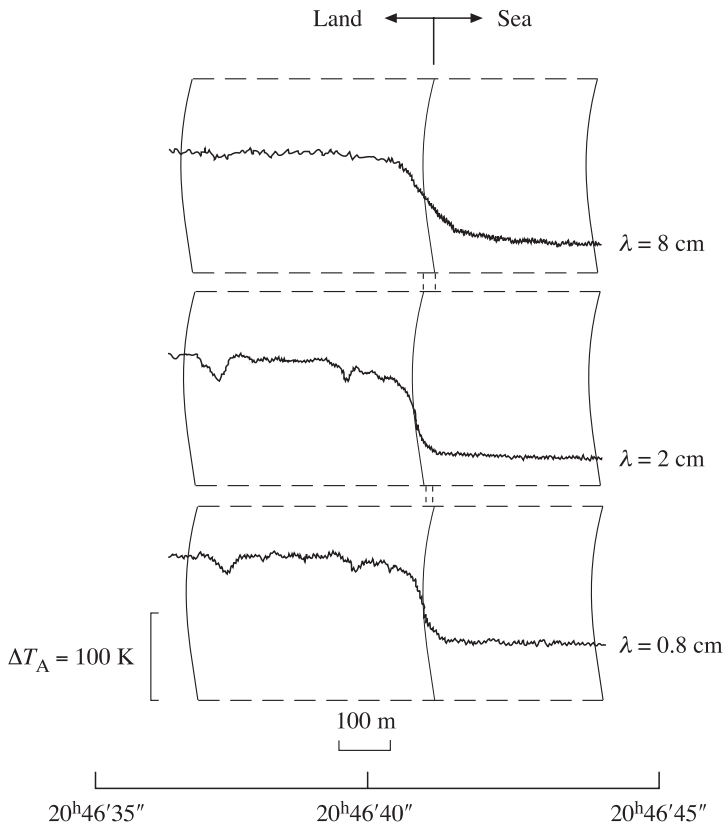


**Figure 5.19.** Fragments of synchronous output signals of airborne radiometers R8, R2 and R0.8 when crossing a land–sea transition. The working area is the Barents Sea, the Cape of Kanin Nose (13 July 1976; $H = 400$ m). Moscow time and indoor temperature calibration are shown on abscissa and on ordinate.

microwave instruments, produced at the Space Research Institute of the Russian Academy of Sciences, which underwent flight tests in 1975–1976 (see Chapter 14). The basic characteristics of radiothermal microwave airborne instruments of the Russian IL-18 aircraft-laboratory are presented in Table 5.2. Note that the table presents the data on the normalized fluctuation threshold sensitivity of instruments, measured directly under onboard conditions. The table also gives the numerical estimates of angular characteristics of the ADP main lobe, obtained in accordance with theoretical concepts (see expression (5.14)).

The antenna parameters of instruments have been estimated using a great volume of in-flight data obtained during 1975–1976 in various regions of Russia: Lake Balkhash (April 1975), Lake Ladoga (September 1975), and the Barents Sea (July 1976).

The examples of fragments of registrograms, obtained at the intersection of contrasting land–water surfaces, are given in Figures 5.13 and 5.16 (channel R-2,

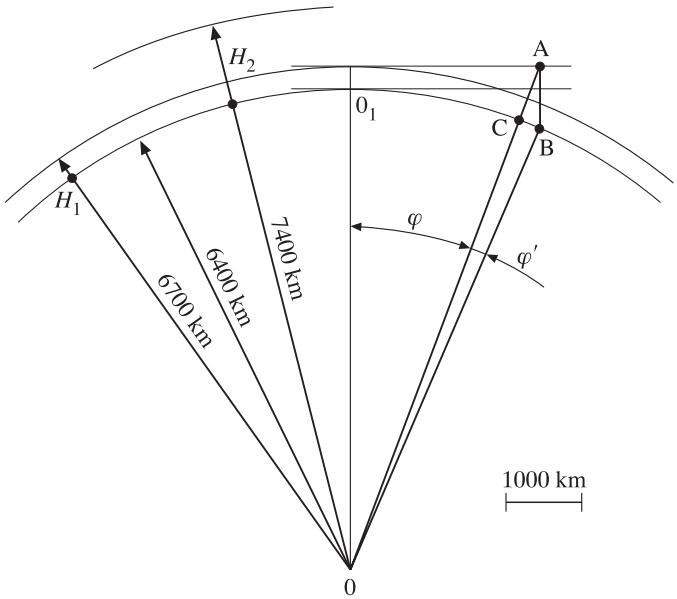


**Figure 5.20.** Scheme of satellite experiment geometry (longitudinal section in orbit plane). $H_1 = 300$ km; $H_2 = 1000$ km. O is the centre of the globe. See the rest of the notation in the text.

wavelength of 2 cm) and in Figures 5.14 and 5.15 (channel R-18, wavelength of 18 cm). Figure 5.20 shows the fragment of synchronous registrograms for channels R-8 (wavelength of 8 cm), R-2 and R-0.8 (wavelength of 0.8 cm). The analysis of registrograms indicates that, as the aircraft altitude increases (from 200 to 4000 m), the degree of discrimination in the registrogram details increases (for the given aircraft velocity and registrator recording rate). The altitudes of 2000–4000 m were found to be most favourable from the viewpoint of discriminating the registrogram details and their subsequent analysis for airborne instruments. The results of registrograms processing in accordance with the MCH method are presented in Table 5.3. The analysis of the table shows good correspondence between calculated and measured (by the proposed technique) ADP main lobe widths for channels R-8 and R-18. At the same time, considerable (1.5-fold) discrepancies between the measured main lobe widths for the R-2 channel are observed. This circumstance was related to design features of the antenna mounting onboard the aircraft, specifically, to the mechanical displacement of the irradiator from the centre of the parabola and, as a consequence, to incomplete use of the aperture area. It was impossible to reveal this circumstance before flight tests under ground conditions.

Using synchronous registrograms of several channels (Figure 5.20), the geometry of the position of the main lobes' axes was calculated (see Figures 5.18 and 5.19). Noticeable displacements of the main lobes' axes of various channels are

related to the features of the mechanical installation of antennas onboard the aircraft, and these features should be taken into account in performing fine spatial experiments.

Another processing problem consisted in the experimental estimation of a scattering coefficient for antennas of the spectral bands used. It follows from the analysis of Table 5.3 that the antenna systems did not have a high value of efficiency: the scattering coefficient values varied from 0.21 to 0.31 for various antennas. It should be emphasized that at this stage of experimental works no special measures were undertaken to decrease the side-lobe radiation of standard antenna systems. Some variations of the scattering coefficient value for the antenna of the R-18 channel, measured at different seasons of years 1975–1976, were caused by design modifications, which took place at antenna mounting.

The most interesting point here is the feature of side-lobe radiation by the antenna system for the R-2 channel. The onboard experiments revealed the obvious anisotropy (Figures 5.13 and 5.16) in the zones of this antenna radiation into the forward and backward hemispheres (with respect to the velocity vector of an aircraft). Using the considered technique (see expression (5.88)), we can obtain values of the scattering coefficient over the forward ($\beta_F$) and backward ($\beta_B$) half-space for the antenna of the R-2 channel:

$$\beta_F = 0.17 \pm 0.01; \beta_B = 0.095 \pm 0.005. \tag{5.97}$$

The physical reason for such a sharp anisotropy of side-lobe radiation is the aforementioned displacement of an irradiator from the focal point of a parabola for design reasons. Of course, it is obviously impossible to reveal such fine features of side-lobe radiation under ground-based tests.

## 5.10 ANTENNA PARAMETERS OF SATELLITE MICROWAVE INSTRUMENTS

The MCH method, developed in section 5.8 for the determination of antenna system parameters for microwave instruments, can be successfully used for measuring the indicated parameters of space systems as well. The only additional point in such applications is the problem of taking into account the sphericity of an experiment, which is schematically presented (in a reduced scale) in Figure 5.21 for spacecraft orbital altitudes of 300 km and 1000 km. It can be seen from this drawing, that the distinctions between plane-parallel and spherical geometries can be characterized by the ratio:

$$\frac{O_1B - O_1C}{O_1C} = \frac{(\varphi - \varphi')R - \varphi R}{\varphi R} = \frac{\varphi'}{\varphi} \tag{5.98}$$

It follows from trigonometric relations, that

$$\frac{\varphi'}{\varphi} = \frac{2}{\varphi}\operatorname{arctg}\frac{R+H}{2R}\operatorname{tg}\varphi - 1. \tag{5.99}$$

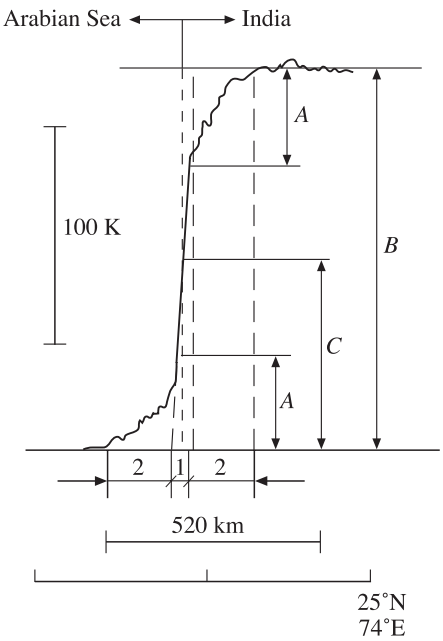


**Figure 5.21.** Fragment of radiometer ($\lambda = 3.4$ cm) output signal of satellite (Russian 'Kosmos-243') instruments when crossing India–Arabian Sea transition (24 September 1968). Spatial scale and indoor temperature calibration are shown in figure. See notation in Figure 5.17.

For small values of angle $\varphi$ and, accordingly, for small distances on the Earth's surface (the $10^\circ$ variation of angle $\varphi$ corresponds to 1000 km on the Earth's surface) we obtain:

$$\frac{\varphi'}{\varphi} = \frac{CB}{O_1C} \approx \frac{H}{R}. \tag{5.100}$$

Thus, it is clear from geometrical considerations, that the noticeable distinctions from planar geometry (for example, when $CB$ will be equal to some resolution elements) can take place for the following spatial size of an investigated area on the Earth's surface:

$$O_1C = \frac{CB}{H/R} = \frac{200}{H/R}. \tag{5.101}$$

So, for $H = 300$ km (the 'Cosmos-243' satellite) $O_1C$ will be 5000 km, and for $H = 1000$ km (the 'Nimbus-5' satellite) $O_1C$ will be 1300 km.

Within the limits of 50–200 km, however, the sphericity of the problem can be neglected, since the distortions will be less than the instantaneous field of resolution of microwave satellite instruments ($CB < 8$ km for the 'Cosmos-243' satellite and less than 17 km for the 'Nimbus-5' satellite).

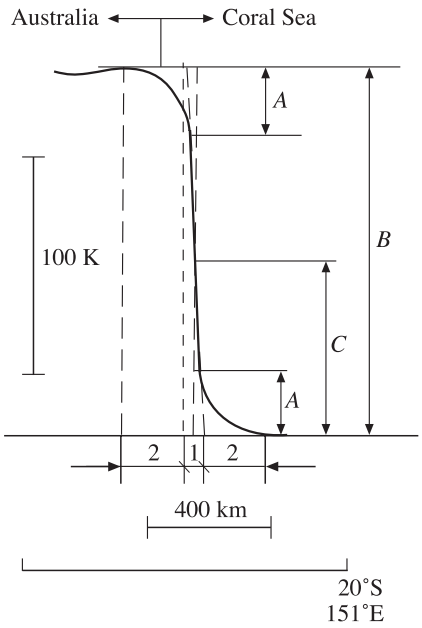


**Figure 5.22.** Fragment of radiometer ($\lambda = 8.5$ cm) output signal of satellite 'Kosmos-243' instruments when crossing Australia–Coral Sea transition (25 September 1968). See notation in Figure 5.21.

To determine the parameters of space antenna systems we have used the available (in the literature) registrograms of land–ocean transitions for microwave instruments of the 'Cosmos-243' and 'Cosmos-384' satellites (Basharinov *et al.*, 1969, 1971, 1973, 1974) and of the 'Nimbus-5' satellite (Vinogradov, 1976). Some characteristics of radiothermal satellite instruments are presented in Table 5.4. Note that the scattering coefficient values for antennas were taken from the data of laboratory (ground and pre-flight) tests. The registrograms of land–ocean transitions, with characteristic regions of brightness temperature variation drawn on them (as it was done in Figure 5.17), and the geographical coordinates are presented in Figures 5.22–5.24.

The analysis of Table 5.4 indicates that the accuracy of main lobe width determination is 10% better than the widths measured under Earth conditions, and for the 'Nimbus-5' antenna the data almost exactly coincide. The only exception is the result of the processing of the transition on 10 December 1970, in the region with coordinates of 80°N lat. and 13°E long. (6.0° as compared to 4.0°), which is explained by the 'spread' character of radiothermal background of the land–ocean transition, rather than by the main lobe width of ADP. As would be expected, the scattering coefficient values for antennas of the 'Cosmos-243' and 'Cosmos-384' satellites obtained from the results of the processing of the land–ocean transitions, are almost 2–2.5 times greater than the values obtained in the laboratory. At the

**Table 5.4.** Antenna parameters of satellite microwave instruments

| Spacecraft (launch year) | Orbit height, km | Time experiments | Positions of land–ocean transition | Working wavelength, cm | Antenna type | $\Delta X$, km | $\theta^*_{3dB}$, degree | $\theta_{3dB}$, degree | $\beta^*$ | $\beta$ (measured) |
|---|---|---|---|---|---|---|---|---|---|---|
| 'Cosmos-243' (1968) | 210–319 | 24 September 1968 | 20°<br>151° | 8.5 | HP | 30–50 | 8.5 | 6.5 | 0.2 | $0.28 \pm 0.05$ |
| | | | 25°<br>74° | 3.4 | HP | 15–25 | 4.0 | 4.3 | 0.15 | $0.32 \pm 0.05$ |
| 'Cosmos-384' (1970) | 212–314 | 10 December 1970 | 35°<br>5° | 3.4 | HP | 15–25 | 4.0 | 4.5 | 0.15 | $0.30 \pm 0.05$ |
| | | | 8°<br>13° | 3.4 | HP | 15–25 | 4.0 | 4.8 | 0.15 | $0.25 \pm 0.05$ |
| 'Nimbus-5' (1972) | 1008–1043 | September 1973 | — | 1.55 | CPA | 25 | 1.6 | 1.57 | — | $0.15 \pm 0.05$ |

HP, horn parabolic antenna; CPA, cophased array with electronic scanning. $\beta^*$ and $\theta^*$ are values of scattering coefficient and ADP main lobe, obtained by laboratory test; $\Delta X$ is special pixel on terrestrial surface.

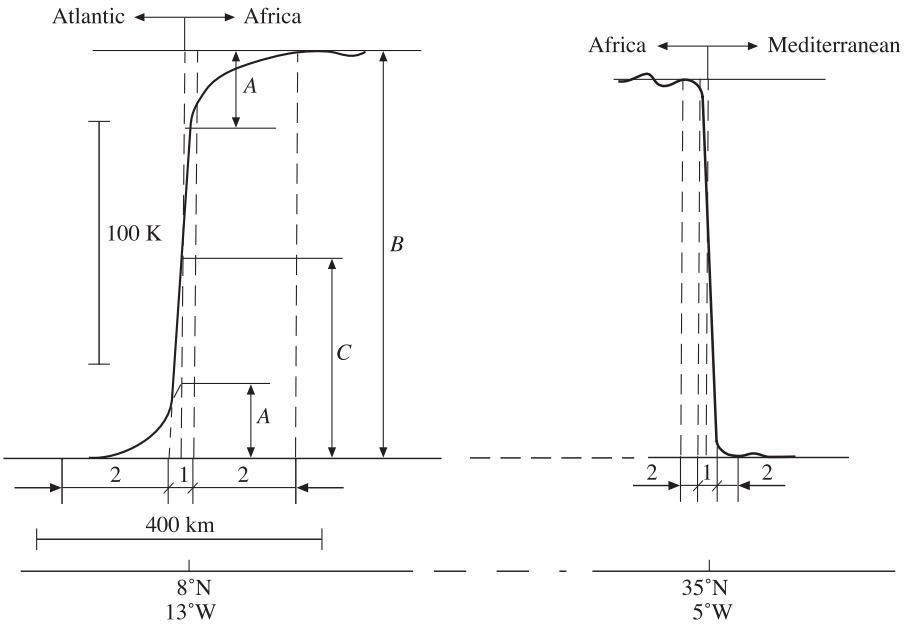


**Figure 5.23.** Fragment of radiometer ($\lambda = 3.4$ cm) output signal of satellite Russian 'Kosmos-384' instruments when crossing Africa (10 December 1970). See notation in Figure 5.17.

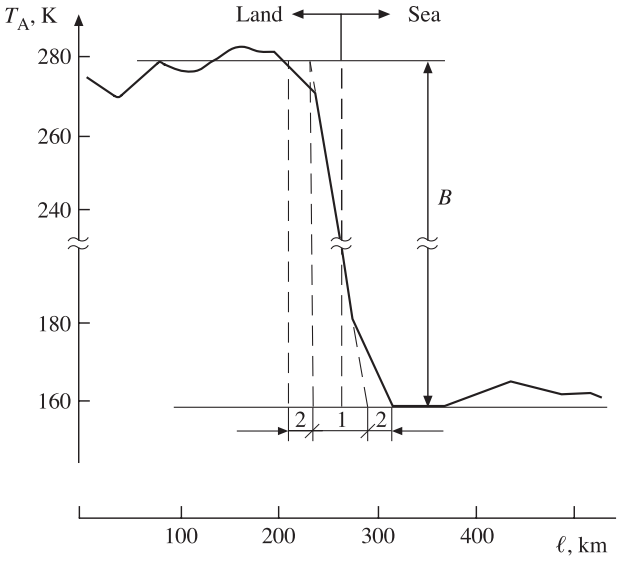


**Figure 5.24.** Fragment of radiometer ($\lambda = 1.55$ cm) output signal of satellite 'Nimbus-5' radiometric instruments when crossing land–sea transition (September 1973). See notation B, 1, 2 in the text.

same time, the phased array of the 'Nimbus-5' satellite demonstrates fairly high values of scattering coefficient. Thus, in general, the scattering coefficient values obtained from the laboratory data (for example, Mo (1999)) cannot reflect the real flight situation at all.

The indicated examples testify to the possibility of using the proposed technique for determining the antenna parameters of radiothermal satellite instruments in flight condition (under the condition of detailed signal recording at the transition of a sharp boundary of contrasting surfaces).